Western diet consumption impairs memory function via dysregulated hippocampus acetylcholine signaling

Anna M.R. Hayes [a], Logan Tierno Lauer [a], Alicia E. Kao [a], Shan Sun [b], Molly E. Klug [a], Linda Tsan [a,c], Jessica J. Rea [a,c], Keshav S. Subramanian [a,c], Cindy Gu [a], Natalie Tanios [a], Arun Ahuja [a], Kristen N. Donohue [a], Léa Décarie-Spain [a], Anthony A. Fodor [b], Scott E. Kanoski [a,c,*]

[a] *Human and Evolutionary Biology Section, Department of Biological Sciences, University of Southern California, Los Angeles, CA, USA*
[b] *Department of Bioinformatics and Genomics, University of North Carolina at Charlotte, Charlotte, NC, USA*
[c] *Neuroscience Graduate Program, University of Southern California, Los Angeles, CA, USA*

ARTICLE INFO

ABSTRACT

Western diet (WD) consumption during early life developmental periods is associated with impaired memory function, particularly for hippocampus (HPC)-dependent processes. We developed an early life WD rodent model associated with long-lasting HPC dysfunction to investigate the neurobiological mechanisms mediating these effects. Rats received either a cafeteria-style WD (*ad libitum* access to various high-fat/high-sugar foods; CAF) or standard healthy chow (CTL) during the juvenile and adolescent stages (postnatal days 26–56). Behavioral and metabolic assessments were performed both before and after a healthy diet intervention period beginning at early adulthood. Results revealed HPC-dependent contextual episodic memory impairments in CAF rats that persisted despite the healthy diet intervention. Given that dysregulated HPC acetylcholine (ACh) signaling is associated with memory impairments in humans and animal models, we examined protein markers of ACh tone in the dorsal HPC (HPCd) in CAF and CTL rats. Results revealed significantly lower protein levels of vesicular ACh transporter in the HPCd of CAF vs. CTL rats, indicating chronically reduced ACh tone. Using intensity-based ACh sensing fluorescent reporter (iAChSnFr) *in vivo* fiber photometry targeting the HPCd, we next revealed that ACh release during object-contextual novelty recognition was highly predictive of memory performance and was disrupted in CAF vs. CTL rats. Neuropharmacological results showed that alpha 7 nicotinic ACh receptor agonist infusion in the HPCd during training rescued memory deficits in CAF rats. Overall, these findings reveal a functional connection linking early life WD intake with long-lasting dysregulation of HPC ACh signaling, thereby identifying an underlying mechanism for WD-associated memory impairments.

1. Introduction

Consumption of a Western diet (WD), broadly defined as a diet high in processed foods, saturated fat, and simple sugars, is associated with excessive caloric intake, obesity, and metabolic dysfunction (Heinonen et al., 2014; Luo et al., 2016; Shively et al., 2019; Wilson et al., 2007). Independent of these outcomes, WD consumption is also linked with cognitive dysfunction (Francis and Stevenson, 2013; Kanoski and Davidson, 2011; Noble et al., 2017b), especially when consumed during early life periods of development (Hsu et al., 2015; Kendig et al., 2013; Tsan et al., 2021). One region of the brain that is particularly vulnerable

to early life dietary insults is the hippocampus (HPC) (Davidson et al., 2012; Kanoski et al., 2010), known for its key role in mediating episodic memory of previous experiences and the context (e.g., time, place) in which they occurred (Bird and Burgess, 2008; Henke et al., 1999; Jarrard, 1993). An accumulating number of studies in both humans and animal models reveal that habitual WD consumption during early life leads to impairments in HPC-dependent learning and memory function, even absent of metabolic dysfunction or body weight gain (Baym et al., 2014; Clark et al., 2020; Ferreira et al., 2018; Noble et al., 2021; Yang et al., 2019). However, despite these established connections between WD consumption and disrupted memory, the underlying

---

neurobiological mechanisms through which WD during development leads to long-lasting hippocampal dysfunction remain elusive.

WD- and obesity-associated alterations in HPC neural processes have been identified, including reduced levels of brain-derived neurotrophic factor, altered synaptic plasticity, and elevated markers of neuro-inflammation (Hsu et al., 2015; Kanoski, 2012; Kanoski and Davidson, 2011; Molteni et al., 2004; Moser and Pike, 2017; Sobesky et al., 2014). However, very little is understood about the underlying neurotransmitter systems driving these outcomes. The HPC relies on acetylcholine (ACh) neurotransmission, particularly from the medial septum, for proper memory function (Bunce et al., 2004; Fadda et al., 1996; Hasselmo, 2006; Levin et al., 2006) and disrupted ACh signaling is a pathological marker of Alzheimer's disease (AD). There is a close relationship between amyloid β peptide (Aβ) accumulation and cholinergic dysfunction in AD, and Aβ suppresses the synthesis and release of ACh from septal neurons (Haam and Yakel, 2017; Liu et al., 2022; Ma and Qian, 2019). Given the longitudinal associations between WD consumption and AD onset (Wieckowska-Gacek et al., 2021), disturbances in ACh signaling is a candidate mechanism for long-term WD-related memory impairments. Here we evaluate the long-lasting impact of early life WD consumption on HPC-dependent contextual episodic memory, and the extent that behavioral outcomes are mediated by dysregulated HPC ACh signaling.

Dietary factors drastically alter the gut microbiome (David et al., 2014; De Filippo et al., 2010; de La Serre et al., 2010; Noble et al., 2017a; Noble et al., 2021; Tsan et al., 2022b) and a growing body of evidence supports a functional link between early life diet, cognitive function, and changes in gut bacteria (Noble et al., 2017b; Noble et al., 2021; Olson et al., 2021). Based on this recent literature, including findings that WD-induced microbiome changes are associated with changes in brain acetylcholine (ACh) signaling (Guo et al., 2021), a plausible hypothesis is that the gut microbiome is functionally connected with early life WD-induced memory impairments, and potentially via changes in HPC ACh function. This hypothesis is evaluated here using an ethologically-relevant WD model that includes dietary choice (between various high sugar and/or fat food and drink options) and macronutrient profiles modeling a modern human WD.

The extent that WD-induced memory impairments are reversible with dietary intervention is poorly understood. In adults, hippocampal-dependent memory impairments induced by a high-fat diet are reversible with healthy diet intervention (Sobesky et al., 2014). However, whether this is also the case following WD consumption during development is poorly understood. Here, we aimed to elucidate how consumption of a WD in early life perturbs memory function in both the short- and long-term. Using our 'junk food' cafeteria-style diet model to represent an early life WD model in rats, we examined metabolic, behavioral, microbial, biochemical, and functional imaging outcomes after a WD access period from juvenile onset, as well as after a healthy diet intervention period starting in early adulthood. Our collective findings show that consumption of a WD in early life leads to long-lasting deficits in HPC-dependent episodic memory that are attributable to impaired HPC ACh signaling, which persist despite a healthy diet intervention in adulthood.

2. Materials and methods

2.1. Subjects

The subjects for all experiments were male Sprague Dawley rats obtained from Envigo (Indianapolis, IN, USA) and housed in the animal vivarium at the University of Southern California. Rats arrived at the animal facility on postnatal day (PN) 25 and started their respective diet on PN 26. They were housed under a reverse 12:12 h light–dark cycle, with lights turned off at 11:00 and turned on at 23:00, and with temperature of 22–24 °C and humidity of 40–50 %. All rats were singly housed in hanging wire cages in order to facilitate food spillage

collection for accurate measurement of individual food intake. Animals were weighed three times per week between 8:30–10:30 (shortly before the onset of the dark cycle). The specific numbers of animals used in each experiment are provided in the general experimental overview below as well as in Supplementary Table S1. All animal procedures were approved by the University of Southern California Institutional Animal Care and Use Committee (IACUC) in accordance with the National Research Council Guide for the Care and Use of Laboratory Animals.

2.2. Dietary model

We implemented a junk food cafeteria-style diet (CAF) to model a Western diet in the present experiments, a model that we previously developed in female rats (Tsan et al., 2022b). This CAF diet consisted of free-choice *ad libitum* access to high-fat high-sugar chow (HFHS diet; D12415, Research Diets, New Brunswick, NJ, USA; 20 % kcal from protein, 35 % kcal from carbohydrate, 45 % kcal from fat), potato chips (Ruffles Original, Frito Lay, Casa Grande, AZ, USA), chocolate-covered peanut butter cups (Reese's Minis Unwrapped, The Hershey Company, Hershey, PA, USA), and 11 % weight/volume (w/v) high-fructose corn syrup-55 (HFCS) beverage (Best Flavors, Orange, CA, USA), placed in separate food/drink receptacles in the home cage for each animal. The 11 % w/v concentration of HFCS was chosen to match the amount of sugar in sugar-sweetened beverages commonly consumed by humans, as we have previously modeled (Hsu et al., 2015; Noble et al., 2019; Tsan et al., 2022b). CAF rats also received *ad libitum* access to water. Control (CTL) rats received the same number of food/drink receptacles, but they were filled with standard chow only (LabDiet 5001; PMI Nutrition International, Brentwood, MO, USA; 28.5 % kcal from protein, 13.5 % kcal from fat, 58.0 % kcal from carbohydrate) or water, accordingly. Body weights and food intakes (including spillage collected on cardboard under the hanging wire cages) were measured three times per week between 8:30–10:30 (shortly before the onset of the dark cycle).

The percentage of total kilocalories consumed from each of the CAF diet components was calculated by multiplying the measured weights of food/drink consumed per rat by the energy density of each component (4.7 kcal/g for HFHS diet, 5.7 kcal/g for potato chips, 5.1 kcal/g for peanut butter cups, 0.296 kcal/g for HFCS beverage), and in the same manner the total energy intake for the CTL group was calculated using the energy density of standard chow (3.36 kcal/g). The percentage of kilocalories consumed from each macronutrient (% kcal from carbohydrate, % kcal from protein, % kcal from fat) for the CAF diet groups was calculated using the kilocalories consumed from each CAF diet component and each component's macronutrient composition.

2.3. General experimental overview

In order to match initial body weights by group in all cohorts, on PN 26 rats were pseudo-randomly assigned to groups receiving either the CAF diet, modeling a WD, or CTL diet from PN 26–56, which approximately represents the juvenile and adolescent periods in rats (Quinn, 2005; Sengupta, 2013). For the first cohort of rats, the WD access period continued until the end of the first time point of behavioral and metabolic assessments (PN 86; 60 days of exposure). After it was established that the memory impairments persisted even after a 30-day healthy diet in the first cohort, subsequent cohorts received WD until PN 56 (30 days). A generalized timeline of procedures is provided in Fig. 1A, and specific details for each of the four experimental cohorts can be found in Supplementary Methods and Materials.

2.4. Metabolic assessments

All metabolic assessments were performed during the dark cycle between 11:00–14:00, and specific methodological details can be found in the Supplementary Materials and Methods file.
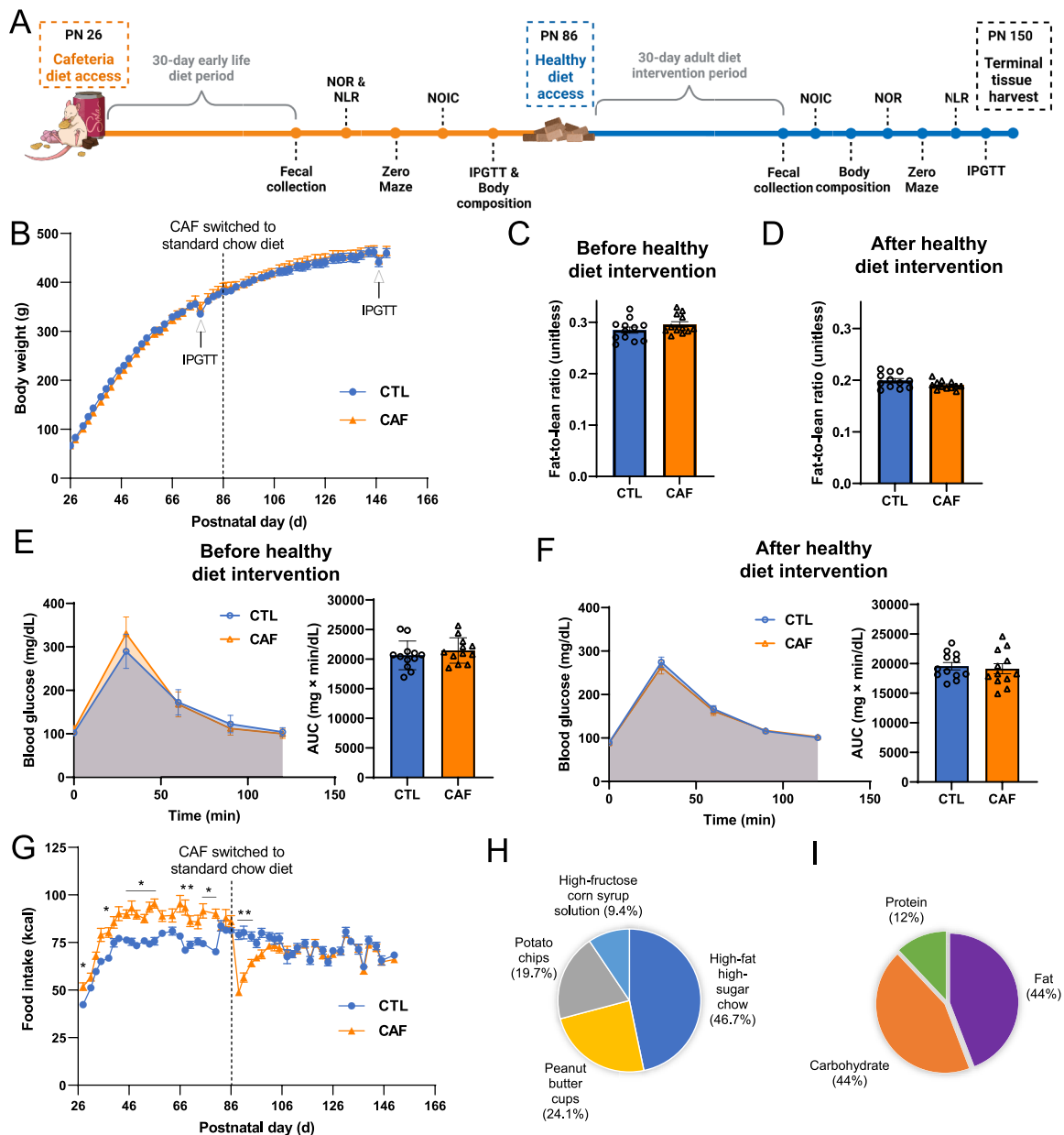
Fig. 1. Early life Western diet consumption does not result in immediate or persistent alterations in body weight trajectory, body composition, or glucose tolerance, despite promoting hyperphagia during the Western diet (WD) period. (A) Experimental design timeline for behavioral and metabolic assessments. (B) Body weight over time (postnatal day) throughout the course of study for the main metabolic and behavioral cohort (N = 24 total rats, n = 12 CTL, n = 12 CAF; two-way ANOVA with repeated measures over time; time × diet: P = 0.0004, no post hoc differences using Sidak's multiple comparisons test, time: P < 0.0001, diet: P = 0.8772; additional cohorts are shown in Fig. S1). (C) Assessment of body composition (fat-to-lean ratio) following the WD period but before the healthy diet intervention (N = 24 total rats, n = 12 CTL, n = 12 CAF; unpaired *t*-test [2-tailed]; P = 0.0766; additional body composition values can be found in Fig. S2). (D) Assessment of body composition (fat-to-lean ratio) following the healthy diet intervention (N = 24 total rats, n = 12 CTL, n = 12 CAF; unpaired *t*-test [2-tailed]; P = 0.1834; additional body composition values can be found in Fig. S2). (E) Glucose tolerance test results after the WD period but before the healthy diet intervention (N = 24 total rats, n = 12 CTL, n = 12 CAF; two-way ANOVA (diet, time [as repeated measure], diet × time interaction) for blood glucose over time; unpaired *t*-test [2-tailed] for blood glucose AUC; time × diet: P < 0.0001, no post hoc differences using Sidak's multiple comparisons test, time: P < 0.0001, diet: P = 0.3812, for AUC: P = 0.3861). (F) Glucose tolerance test results following the healthy diet intervention (N = 24 total rats, n = 12 CTL, n = 12 CAF; two-way ANOVA (diet, time [as repeated measure], diet × time interaction) for blood glucose over time; unpaired *t*-test [2-tailed] for blood glucose AUC; time × diet: P = 0.8630, time: P < 0.0001, diet: P = 0.7111, for AUC: P = 0.6909). (G) Food intake expressed as kcal over time (postnatal day) throughout the course of study for the main metabolic and behavioral cohort (N = 24 total rats, n = 12 CTL, n = 12 CAF; two-way ANOVA with repeated measures over time; time × diet: P < 0.0001, many post hoc differences using Sidak's multiple comparisons test, time: P < 0.0001, diet: P = 0.0479; additional cohorts are shown in Fig. S1). (H) Percentage of energy intake consumed from the CAF diet components for the main metabolic and behavioral cohort (N = 24 total rats, n = 12 CTL, n = 12 CAF; additional cohorts are shown in Fig. S1). (I) Percentage of energy intake from macronutrients for the main metabolic and behavioral cohort (N = 24 total rats, n = 12 CTL, n = 12 CAF; additional cohorts are shown in Fig. S2). AUC, area under the curve; CAF, cafeteria diet group; CTL, control group; WD, Western diet. Error bars represent ± SEM. *P < 0.05, **P < 0.01.

2.5. Behavioral assessments

All behavioral assessments were performed during the dark cycle between 11:00 and 17:00.

2.5.1. Novel location recognition (NLR)

NLR was performed to assess spatial recognition memory, which relies on HPC function (Broadbent et al., 2004; Clark et al., 2005). A grey opaque box (38.1 cm L × 56.5 cm W × 31.8 cm H), placed in a dimly lit room in which two adjacent desk lamps were pointed toward the floor, was used as the NLR apparatus. Rats were habituated to the empty apparatus and conditions for 10 min 1–2 days prior to testing. Testing constituted a 5-min familiarization phase during which rats were placed in the center of the apparatus (facing a neutral wall to avoid biasing them toward either object) with two identical objects placed in two corners of the apparatus and allowed to explore. The objects used were either two identical empty glass salt-shakers (that never contained salt) or two identical empty soap dispensers (that were never used with soap; first NLR time point), or two identical textured glass vases or two identical ceramic jugs (second NLR time point). Rats were then removed from the apparatus and placed in their home cage for 5 min. During this period, the apparatus and objects were cleaned with 10 % ethanol solution and one of the objects was moved to a different corner location in the apparatus (i.e., the object was moved but not replaced). Rats were then placed in the center of the apparatus again and allowed to explore for 3 min. The types of objects used and the novel location placements were counterbalanced by group. The time each rat spent exploring the objects was quantified by hand-scoring of video recordings by an experimenter blinded to the animal group assignments, and object exploration was defined as the rat sniffing or touching the object with the nose or forepaws.

2.5.2. Novel object in context (NOIC)

NOIC was conducted to assess HPC-dependent contextual episodic memory (Balderas et al., 2008; Martínez et al., 2014). The 5-day NOIC procedure was adapted from previous research (Martínez et al., 2014), and conducted as in previous work from our laboratory (Davis et al., 2020; Noble et al., 2021; Suarez et al., 2018; Tsan et al., 2022a; Tsan et al., 2022b). Each day consisted of one 5-min session per animal, with cleaning of the apparatus and objects using 10 % ethanol between each animal. Days 1 and 2 were habituation to the contexts – rats were placed in Context 1, a semitransparent box (41.9 cm L × 41.9 cm W × 38.1 cm H) with yellow stripes, or Context 2, a black opaque box (38.1 cm L × 63.5 cm W × 35.6 cm H). Each context was presented in a distinct room, both with similar dim ambient lighting yet with distinct extra-box contextual features. Rats were exposed to one context per day in a counterbalanced order per diet group for habituation. Following these two habituation days, on the next day each animal was placed in Context 1 containing single copies of Object A and Object B situated on diagonal equidistant markings with sufficient space for the rat to circle the objects (NOIC day 1). Objects were an assortment of hard plastic containers, tin canisters (with covers), and the Original Magic 8-Ball (two types of objects were used per experimental cohort time point; objects were distinct from what animals were exposed to in NOR and NLR). The sides where the objects were situated were counterbalanced per rat by diet group. On the following day (NOIC day 2), rats were placed in Context 2 with duplicate copies of Object A. The next day was the test day (NOIC day 3), during which rats were placed in Context 2 again, but with single copies of Object A and Object B; Object B was therefore not a novel object, but its placement in Context 2 was novel to the rat. Each time the rats were situated in the contexts, care was taken so that they were consistently placed with their head facing away from both of the objects. On NOIC days 1 and 3, object exploration, defined as the rat sniffing or touching the object with the nose or forepaws, was quantified by hand-scoring of videos by an experimenter blinded to the animal group assignments. The discrimination index for Object B was calculated for

NOIC days 1 and 3 as follows: time spent exploring Object B (the "novel object in context" in Context 2)/[time spent exploring Object A + time spent exploring Object B]. Data were then expressed as a percent shift from baseline as: [day 3 discrimination index − day 1 discrimination index] × 100. Rats with intact HPC function will preferentially explore the "novel object in context" on NOIC day 3, while HPC impairment will impede such preferential exploration (Balderas et al., 2008; Martínez et al., 2014).

Methods for Novel Object Recognition (NOR), Zero Maze, and Open Field are found in Supplementary Methods and Materials.

2.6. Stereotaxic surgery

Stereotaxic surgery procedures are found in the Supplementary Methods and Materials file.

2.7. In vivo fiber photometry during memory testing

Fiber photometry during NOIC procedure and data analyses. Fiber photometry involves transmission of a fluorescence light through an optical patch cord (Doric Lenses, Quebec City, Quebec, Canada) and convergence onto the optic fibers implanted in the animals, which in turn emits neural fluorescence through the same optic fibers/patch cords and is focused on a photoreceiver. For the present experiments, animals were habituated to having patch cords attached to their HPC fiber optic cannulae prior to NOIC experimentation. Every animal had patch cords attached for both NOIC habituation days as well NOIC days 1–3, and unilateral photometry recordings were collected on NOIC days 1 and 3. Recording sessions lasted the duration of the trials on both NOIC days 1 and 3 (5 min each day per rat). Photometry signal was captured according to previous work by our group using the Neurophotometrics fiber photometry system (Neurophotometrics, San Diego, CA, USA) at a sampling frequency of 40 Hz with alternating wavelengths at 470 nm and 415 nm (Décarie-Spain et al., 2022; Subramanian et al., 2023). The signal representing ACh release (470 nm) was corrected by subtracting the isosbestic signal (415 nm) and fitting the result to a biexponential curve using MATLAB (R202a, MathWorks, Inc., Natick, MA, USA). Corrected fluorescence signal was normalized within each recording session per rat by calculating ΔF/F using the average fluorescence signal for the entire recording. Resulting data was aligned with real-time location of each animal obtained from ANYmaze behavior tracking software (Stoelting, Wood Dale, IL, USA) using a customized MATLAB code. Investigations occurring at least 5 s apart were isolated for further analysis. Time-locked z-scores were obtained by normalizing ΔF/F for the 5 s following an object investigation episode to the ΔF/F at the onset of the investigation (time 0 s). Area under the curve was also calculated for z-scores for the 5 s following an object investigation episode. Aside from the patch cords and recording, NOIC was performed in the same manner as detailed above.

2.8. HPC ACh agonist infusion during memory testing

Animals were habituated to having their cannulae obturators removed and replaced one week prior to NOIC experimentation. Injectors for drug administration projected 1 mm beyond the guide cannulae for all infusions. NOIC procedures were carried out as described above with the exception that infusions of either ACh agonist or vehicle were performed in the animal housing room 3–8 min before each animal was placed in Context 2 on NOIC day 2 for the 5-min familiarization period with duplicate copies of Object A. This agonist administration timing was based off previous research (Caine et al., 1991) and pilot experiments in our lab that identified the encoding and consolidation periods as critical to ACh function (data not shown). The broad, nonselective ACh agonist carbachol (0.8 μg total dose; 0.2 μL volume of 2 μg/μL per side; Y0000113, Millipore Sigma, St. Louis, MO, USA), the α7 nAChR specific agonist PNU 282987 (1.6 μg total dose; 0.2

μL volume of 4 μg/μL per side; PNU 282987, Tocris, Ellisville, MO, USA), or vehicle (artificial cerebrospinal fluid [aCSF] or 50/50 % aCSF/dimethylsulfoxide [DMSO]) was infused bilaterally per rat. Volumes for bilateral HPC infusions were 200 nl/hemisphere (rate = 5 μL/min) via a 33-gauge injector and microsyringe attached to an infusion pump (Harvard Apparatus). Injectors were left in place for 20 s after infusions. Carbachol was dissolved in aCSF, and PNU 282987 was dissolved in 50/50 % aCSF/DMSO. Following infusions, animals were carefully brought to the behavior room and proceeded with NOIC day 2 training as described above.

2.9. Tissue collection

2.9.1. Experimental cohorts 1 and 2

Following intramuscular injection of a cocktail of ketamine (90.1 mg/kg body weight), xylazine (2.8 mg/kg body weight), and acepromazine (0.72 mg/kg body weight), animals were rapidly decapitated. Cecal content was collected as described below, and brains were flash-frozen in a beaker containing −30 °C isopentane, surrounded by dry ice. All samples were stored at −80 °C until further processing and analysis. Tissue punches of the dorsal HPC (atlas levels 28–32; one 2 mm diameter punch in the CA1 / dentate gyrus, one 1 mm diameter punch in the CA3) for immunoblot analyses were collected using the Leica CM cryostat (Wetzlar, Germany) and anatomical landmarks were based on the Swanson rat brain atlas (Swanson, 2018). Punches were stored at −80 °C until used for later immunoblotting assays as described below.

2.9.2. Experimental cohort 3

Rats were anesthetized via an intramuscular injection of a ketamine (90.1 mg/kg body weight), xylazine (2.8 mg/kg body weight), and acepromazine (0.72 mg/kg body weight) cocktail and then transcardially perfused with 0.9 % sterile saline (pH 7.4) followed by 4 % paraformaldehyde (PFA) in 0.1 M borate buffer (pH 9.5). Brains were dissected from the skull and post-fixed in PFA with 15 % sucrose for 24 h, and then flash-frozen in isopentane cooled in dry ice. Brains were then stored at −80 °C. On a freezing microtome, brains were sectioned to 30 μm thickness and sections were collected in 5-series, stored in antifreeze solution at −20 °C, and thereafter immunohistochemistry was performed to visualize viral expression as described in Supplementary Materials. Photomicrographs for confirmation of AAV injection sites and fiber optic cannulae placement within the dorsal dentate gyrus of the hippocampus were captured using a Nikon 80i camera (Nikon DSQI1, 1280X1024 resolution, 1.45 megapixel) under epifluorescence. 70 % of animals were included in data analysis, taking injection site, cannulae placement, and acquisition of quality signal during photometry recordings into consideration.

2.9.3. Experimental cohort 4

Injection of a cocktail of ketamine (90.1 mg/kg body weight), xylazine (2.8 mg/kg body weight), and acepromazine (0.72 mg/kg body weight) was administered intramuscularly. Pontamine sky blue ink (2 %, 200 nL per hemisphere) was then infused into the indwelling HPC bilateral cannulae to allow for postmortem verification of the infusion sites. Thereafter, rats were rapidly decapitated. Brains were extracted and post-fixed in 10 % formalin until further processing. Cannulae placements were examined through anatomical verification of the position of the pontamine sky blue ink infusions. Animals with ink confined to the dorsal HPC based on the Swanson rat brain atlas (Swanson, 2018) in both cannulae were included in data analysis. 5 % of animals were excluded from data analysis based on this criterion.

2.10. Western blotting (experimental cohort 1)

Dorsal HPC tissue punches from experimental cohort 1 were analyzed for levels of markers of cholinergic tone (choline acetyltransferase [ChAT], vesicular acetylcholine transporter [VAChT], and acetylcholinesterase [AChE]) as well as for levels of key inflammatory markers (Tumor Necrosis Factor-α [TNF-α], interleukin-6 [IL-6], and interleukin-1β [IL-1β]). Proteins in brain lysates (25 μg per sample/well; determined via the reducing agent and detergent compatible [RC DC^{TM}] protein assay, Bio-Rad Laboratories, Inc.) were separated using sodium dodecyl sulfate polyacrylamide gel electrophoresis, transferred onto poly-vinylidene difluoride membranes, and subjected to enhanced chemiluminescence for immunodetection analysis (Chemidoc XRS, BioRad). A rabbit polyclonal anti-choline acetyltransferase antibody (1:100; Sigma-Aldrich, catalog # AB143) was used to determine the concentration of ChAT relative to a load control signal detected by a rabbit anti-β-tubulin antibody (1:1000; Cell Signaling Technology, 9F3 rabbit mAb, catalog # 2128). A rabbit polyclonal anti-vesicular ACh antibody (1:1000; Sigma-Aldrich, catalog # ABN100) was used to determine the concentration of VAChT relative to a load control signal detected by a rabbit anti-β-actin antibody (1:1000; Abcam, catalog # ab8227). A rabbit recombinant anti-acetylcholinesterase antibody (1:1000; Abcam, catalog # ab183591) was used to determine the concentration of AChE relative to a loading control signal detected by a rabbit anti-β-actin antibody (1:1000; Santa Cruz Biotechnology, catalog # NB600-503). A rabbit polyclonal anti-TNF-α antibody (1:1000; Abcam, catalog # ab6671) and rabbit polyclonal anti-IL-1β antibody (1:1000; Abcam, catalog # ab2105) were used to determine the concentrations of TNF-α and IL-1β, respectively, relative to a loading control signal detected by a rabbit anti-β-tubulin antibody (1:1000; Cell Signaling Technology, D13U1W mouse mAb, catalog # 86298). A mouse monoclonal anti-IL-6 antibody (1:1000; Abcam, catalog # ab9423) was used to quantify the concentration of IL-6 relative to a mouse anti-β-tubulin antibody (1:1000; Cell Signaling Technology, 9F3 rabbit mAb, catalog # 2128). Goat anti-rabbit-IgG-horseradish peroxidase (HRP)-linked antibody (1:5000; Cell Signaling Technology, catalog # 7074) was used as the secondary antibody for ChAT, VAChT, AChE, TNF-α, and IL-1β, while sheep ECL anti-mouse-IgG-HRP-linked antibody (1:5000; GE Healthcare UK Limited, catalog # NA931V) was used as the secondary antibody for IL-6. Blots were quantified with densitometry analysis using ImageJ as previously reported (Hsu et al., 2015; Kanoski et al., 2013; Suarez et al., 2018).

2.11. Microbiome analyses

Methodological details for the microbiome analyses can be found in the Supplementary Materials and Methods file.

2.12. Statistical analysis

Data are presented as means ± standard errors (SEM) for error bars in all figures. Each experimental group was analyzed with its respective control group per experimental cohort. Statistical analyses were performed using Prism software (GraphPad, Inc., version 8.4.2, San Diego, CA, USA) or R (4.2.0, R Core Team 2022. Significance was considered at $p < 0.05$. Detailed descriptions of the specific statistical tests per figure panel can be found in Table S1. In all cases, model assumptions were checked (normality by Shapiro-Wilk test and visual inspection of a qq plot for residuals per analysis, equal variance/homoscedasticity by an F test to compare variances and visual inspection of a residual plot per analysis). In one case (NLR time point 1 for cohort 1), data violated the assumption of homoscedasticity and thus a Welch's correction was employed to account for the unequal variance. Group sample sizes were based on prior knowledge gained from extensive experience with rodent behavior testing and survival animal surgeries.

3. Results

3.1. Early life WD does not yield obesity or metabolic impairments

No differences in body weight were observed between CAF and CTL

rats throughout either the WD access period or healthy diet intervention (Fig. 1A and B, Fig. S1C and E). Furthermore, no differences in body composition (lean/fat mass ratio) were observed either after the early life WD access period or after the healthy diet intervention period (Fig. 1C and D, Fig. S2E and F). Glucose tolerance was not altered in CAF rats compared to CTL rats at either time point (Fig. 1E and F). Despite

the lack of body weight and body composition effects, rats receiving the CAF diet in early life consumed approximately 15 % more kilocalories than CTL rats during the early life WD access period. However, this increased caloric intake did not persist when the CAF rats were switched to the healthy diet in adulthood (Fig. 1G; Fig. S1B, D, F). During the WD access period, rats in the CAF group consumed the majority of their
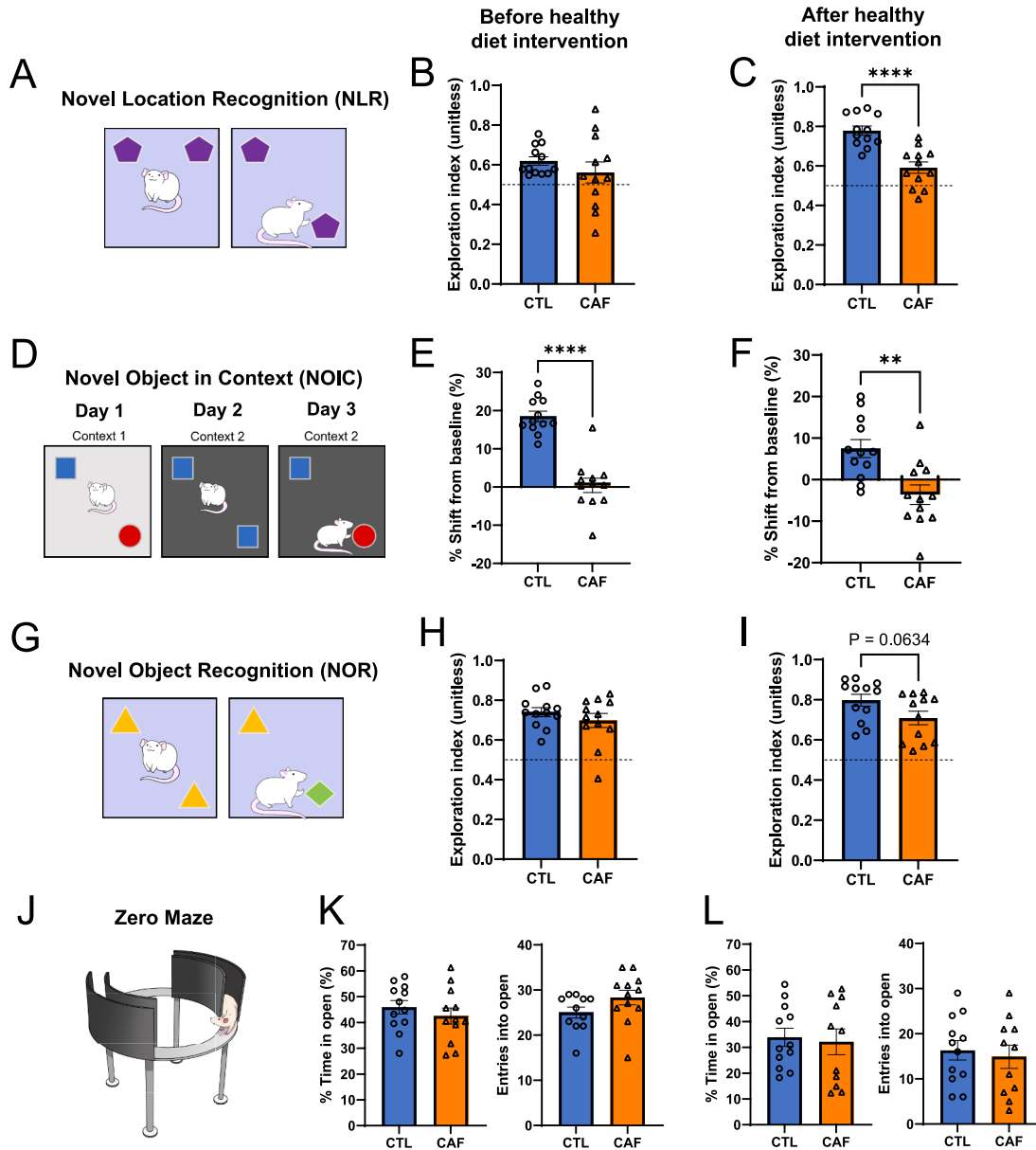
Fig. 2. Early life Western diet (WD) consumption yields long-lasting episodic memory impairments in the absence of impacts on perirhinal cortex-dependent novel object exploration or markers of anxiety. (A) Novel Location Recognition (NLR) behavioral scheme. (B) NLR exploration index following the WD access period but before the healthy diet intervention (N = 24 total, n = 12 CTL, n = 12 CAF; unpaired t-test [2-tailed] with Welch's correction for unequal variances; P = 0.3258). (C) NLR exploration index following the healthy diet intervention (N = 24 total, n = 12 CTL, n = 12 CAF; unpaired t-test [2-tailed]; P < 0.0001). (D) Novel Object in Context (NOIC) behavioral scheme. (E) NOIC percent shift from baseline performance following the WD access period but before the healthy diet intervention (N = 24 total, n = 12 CTL, n = 12 CAF; unpaired t-test [2-tailed]; P < 0.0001). (F) NOIC percent shift from baseline performance following the healthy diet intervention (N = 24 total, n = 12 CTL, n = 12 CAF; unpaired t-test [2-tailed]; P = 0.002). (G) Novel Object Recognition (NOR) behavioral scheme. (H) NOR exploration index following the WD access period but before the healthy diet intervention (N = 24 total, n = 12 CTL, n = 12 CAF; unpaired t-test [2-tailed]; P = 0.3320). (I) NOR exploration index following the healthy diet intervention (N = 24 total, n = 12 CTL, n = 12 CAF; unpaired t-test [2-tailed]; P = 0.0634). (J) Zero Maze apparatus illustration. (K) Percent time spent in and entries into the open arm regions of the Zero Maze apparatus after the WD access period but before the healthy diet intervention (N = 23 total, n = 11 CTL due to one outlier, n = 12 CAF; unpaired t-test [2-tailed]; P = 0.4064 for percent time in open, P = 0.1175 for entries into open). (L) Percent time spent in and entries into the open arm regions of the Zero Maze apparatus following the healthy diet intervention (N = 23 total, n = 12 CTL, n = 11 CAF due to one outlier; unpaired t-test [2-tailed]; P = 0. 7719 for percent time in open, P = 0. 6752 for entries into open). CAF, cafeteria diet group; CTL, control group; WD, Western diet. Error bars represent ± SEM. **P < 0.01, ****P < 0.0001.

kilocalories from the distinct CAF components in the following order (highest to lowest % kcal consumed): high-fat, high-sugar chow > peanut butter cups ≥ potato chips > HFCS (Fig. 1H; Supplementary Fig. S2A–C). In terms of macronutrients during the WD period, CAF rats consumed approximately equal kilocalories (44 %) from fat and carbohydrate, and the remaining from protein (12 %) (Fig. 1I; Fig. S2A–C). For comparison, the healthy standard chow that the CTL group received throughout the study and that the CAF group received for the healthy diet intervention contained 13 %, 58 %, and 29 % kcal from fat, carbohydrate, and protein, respectively. Collectively, these results show that despite promoting overconsumption of energy, the WD model did not induce an obesogenic weight trajectory or metabolic impairments, and the hyperphagia reversed immediately upon healthy diet intervention.

3.2. Early life WD imparts long-lasting HPC-dependent memory impairments without influencing perirhinal cortex-dependent memory or novelty aversion

We performed both Novel Location Recognition (NLR) and Novel Object in Context (NOIC) to assess HPC-dependent spatial recognition (Broadbent et al., 2004; Clark et al., 2005) and contextual episodic memory (Balderas et al., 2008; Martínez et al., 2014), respectively (Fig. 2A–F). Following the early life WD access period, there were no differences in spatial recognition memory evaluated through NLR (Fig. 2B). After the healthy diet intervention period the CAF rats showed an impairment in this task (Fig. 2C). As for NOIC, deficiencies in contextual episodic memory were apparent both before and after the healthy diet intervention period in CAF rats (Fig. 2E and F; Fig. S3), signifying that early life WD consumption led to long-lasting memory impairments, regardless of consumption of a healthier diet in early adulthood. Importantly, these deficits occurred absent of any differences in total object exploration time between the CAF and CTL groups (Fig. S3A–D, F–I). Together, these findings reveal that early life WD 'programs' long-lasting deficits in HPC-dependent memory function.

To evaluate object recognition memory that is not HPC-dependent, we determined whether consumption of a WD in early life impairs memory in a Novel Object Recognition (NOR) behavioral approach that relies on the perirhinal cortex independently of the HPC (Albasser et al., 2011; Cohen and Stackman, 2015) (Fig. 2G). Immediately following the early life WD access period, there were no differences in exploration index of a novel vs. non-novel object between CAF and CTL rats (Fig. 2H; P = 0.33). Following the healthy diet intervention period, there was a trend for decreased exploration of a novel object in CAF rats vs. CTL rats, but this did not reach significance (Fig. 2I; P = 0.06). These findings indicate early life WD consumption did not lead to robust differences in recognition of a novel object in a memory task that does not involve the HPC. Importantly, these results suggest that NLR and NOIC impairments were not secondary to novelty aversion.

3.3. Early life WD does not alter markers of anxiety or locomotor activity

Because memory and anxiety-like behavior can both involve hippocampal function (André et al., 2014; Carlini et al., 2011; Miller and Hen, 2015), we examined markers of anxiety-like behavior and locomotor activity through the Zero Maze and Open Field tests. There were no differences in the percentage of time that rats spent in the open arms of the Zero Maze apparatus, a marker of anxiety-like behavior, between the CAF and CTL groups either before or after the healthy diet intervention (Fig. 2J–L). Furthermore, there were no differences in the number of entries into the open arms of the Zero Maze apparatus at either time point (Fig. 2K and L), which is an assessment of locomotor activity. We also performed the Open Field task after the WD access period, and there were no differences in distance travelled, an additional assessment of locomotor activity, or time spent in the center of the apparatus, an additional marker of anxiety-like behavior, in this test (Fig. S3L and M).

These results signify that the persistent HPC-dependent memory impairments due to a WD are not confounded by altered anxiety-like behavior or locomotor activity.

3.4. Early life WD leads to gut microbiome alterations that are reversed with adult healthy diet intervention

Because the gut microbiome has previously been shown to be altered by WD exposure (Tsan et al., 2022b), we examined whether early life WD consumption impacted gut microbial taxonomic composition both immediately after the WD access period as well as after the healthy diet intervention period. Cladogram visualization and PCoA of 16 s rRNA sequencing of fecal samples collected immediately after the 30-day WD period reveal robust differences in gut microbiome at the genus level between CAF and CTL rats (Fig. 3A and B). Similar differences were observed in the PCoA for sequences of cecal content of animals that were not exposed to the healthy diet intervention (Fig. 3D). However, after the healthy diet intervention, PCoAs of sequences of both fecal and cecal contents revealed that the initial marked differences were largely reversed (Fig. 3C and E). Shannon indices, which assess α-diversity of microbial communities in fecal and cecal samples were significantly lower in the CAF group than those in the CTL group after the early life WD access period, but these differences did not persist after the healthy diet intervention (Fig. S4). A cladogram for the time point after WD exposure depicts the broad distribution of taxa across groups (Fig. 3A). By contrast, only 5 taxa were significantly altered after the healthy diet intervention (FDR < 0.1), further indicating that early life WD did not impart long-lasting effects on the gut microbiome.

Given the pronounced differences in gut microbiome immediately after the early life WD access period, we performed correlation analyses to determine if any microbial taxa were related to the early life WD memory impairments observed. A number of correlational analyses between specific taxon and memory performance in the NOIC task at the time point following the early life WD access period withstood the FDR correction (Fig. S4). Most notably, individual abundances of the genera *Lactococcus* and *Bifidobacterium* were negatively correlated with NOIC memory performance (Fig. S4). In contrast, abundance of the species *Lactobacillus intestinalis* was positively correlated with NOIC memory performance (Fig. S4). We then sought to decipher a potential mechanistic role of the gut microbiome in the long-lasting memory deficits by building a machine learning model to test whether the gut microbiome immediately after the WD access period could predict memory function in NOIC after the healthy diet intervention. Using random forest regression models with both 3-fold and 4-fold cross validation, we observed that microbiome after the WD period was linked with NOIC memory performance before the healthy diet intervention but not later in life after the healthy diet intervention (Fig. 3F, Fig. S5). This indicates that the microbiome was not responsible for the long-lasting memory impairments observed.

3.5. Early life WD yields long-lasting reductions in chronic HPC ACh signaling tone

Given that the HPC relies on ACh neurotransmission for proper memory function (Bunce et al., 2004; Fadda et al., 1996; Hasselmo, 2006; Levin et al., 2006), we examined levels of proteins related to ACh signaling in the HPC as a potential novel mechanism for enduring HPC dysfunction from early life WD. Protein quantification was evaluated for choline acetyltransferase (ChAT), an enzyme that synthesizes ACh from the precursors choline and acetyl-CoA whose expression correlates positively with spatial memory (Dunbar et al., 1993); vesicular ACh transporter (VAChT), which transports ACh to vesicles for synaptic release and whose expression is positively correlated with improved spatial memory function during aging (Nagy and Aubert, 2015); and HPC acetylcholinesterase (AChE), an enzyme that degrades ACh and that has been found to disrupt memory function (Haider et al., 2014;
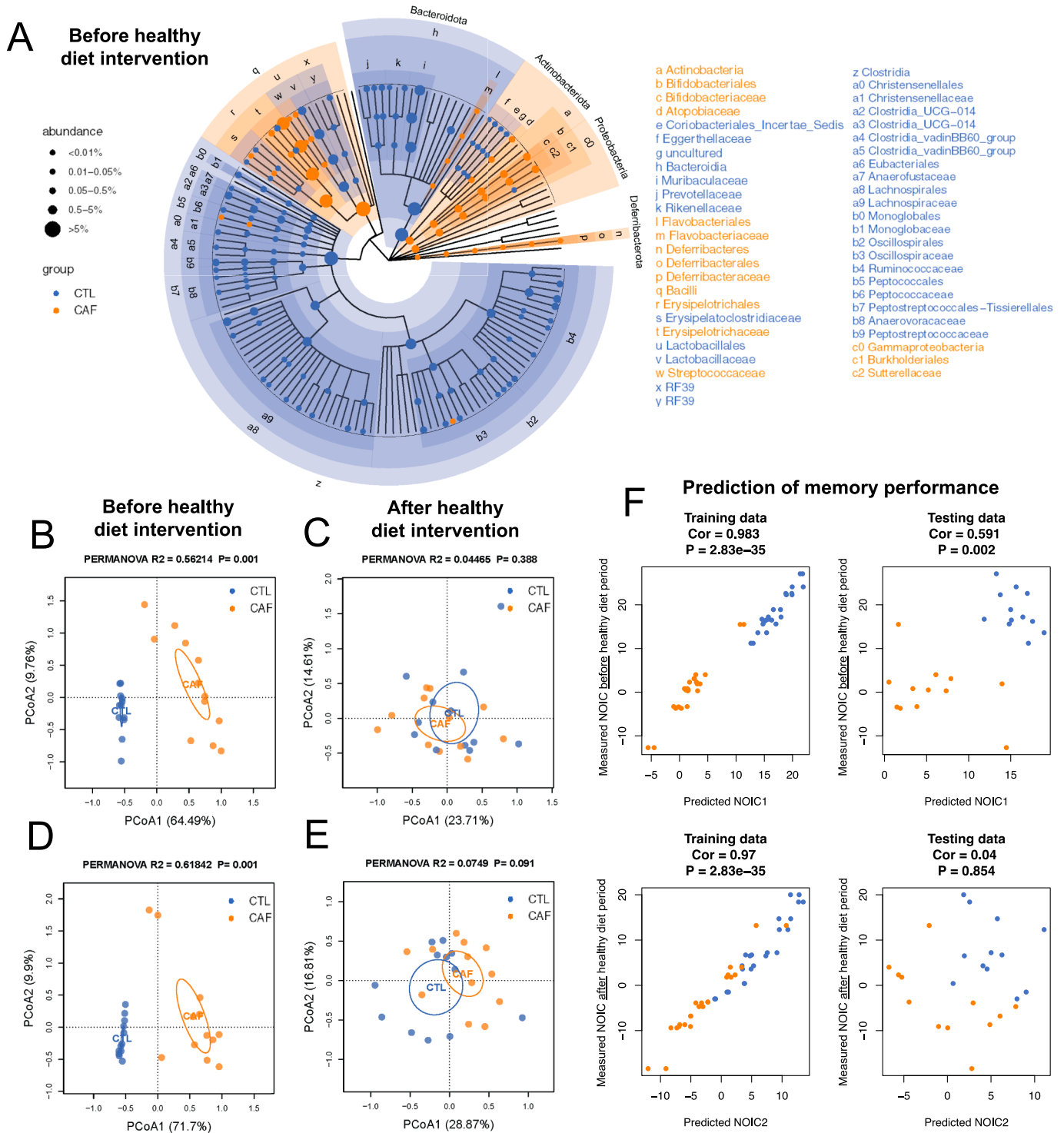
Fig. 3. Early life Western diet (WD) robustly alters the gut microbiome, but these alterations do not persist upon a healthy diet intervention in adulthood. (A) Cladogram representation of differentially abundant taxa in fecal matter after the WD period but before the healthy diet intervention period (N = 24 total, n = 12 CTL, n = 12 CAF; false discovery rate [FDR] < 0.1 for significant taxa). (B) Principal coordinate analysis (PCoA) of microbiomes at the genus level in fecal matter after the WD access period (N = 24 total, n = 12 CTL, n = 12 CAF; Bray-Curtis dissimilarity; PERMANOVA, R^2 = 0.56214, P = 0.001, P < 0.05 for significant associations). (C) PCoA of microbiomes at the genus level in fecal matter after the healthy diet intervention period (N = 24 total, n = 12 CTL, n = 12 CAF; Bray-Curtis dissimilarity; PERMANOVA, R^2 = 0.04465, P = 0.388). (D) PCoA of microbiomes at the genus level in cecal content after the WD access period (N = 24 total, n = 12 CTL, n = 12 CAF; Bray-Curtis dissimilarity; PERMANOVA, R^2 = 0.61842, P = 0.001). (E) PCoA of microbiomes at the genus level in cecal content after the healthy diet intervention period (N = 24 total, n = 12 CTL, n = 12 CAF; Bray-Curtis dissimilarity; PERMANOVA, R^2 = 0.0749, P = 0.388). (F) Machine learning analysis to evaluate whether microbiome composition before the healthy diet intervention period reliably predicts NOIC memory performance either before or after the healthy diet period (N = 24 total, n = 12 CTL, n = 12 CAF; random forest regression models, 3-fold cross validation; for training data: Cor 0.983 and P = 2.83e-35 [before healthy diet intervention period], Cor 0.97 and P = 2.83e-35 [after healthy diet intervention period]; for testing data: Cor 0.591 and P = 0.002 [before healthy diet intervention period], Cor 0.04 and P = 0.854 [after healthy diet intervention period]). CAF, cafeteria diet group; CTL, control group; FDR, false discovery rate; PCoA, principal coordinate analysis; WD, Western diet.

Pepeu and Giovannini, 2010). Immunoblotting analyses from dorsal HPC tissue collected after the healthy diet intervention period revealed that there were no differences in ChAT or AChE levels, yet CAF rats had reduced levels of VAChT compared to CTL rats (Fig. 4A–C). These results suggest that there was no post-synaptic compensation for a reduced amount of ACh reaching a synapse. To further determine whether these changes in chronic cholinergic tone could be related to features of the microbiome, we performed correlational analyses between the abundances of key microbial taxa both before and after the healthy diet intervention and VAChT levels, and results revealed no significant correlations for any taxa (Fig. S6). Overall, these findings suggest that early life WD consumption leads to long-lasting reductions in cholinergic tone.

Previous research has identified a cholinergic anti-inflammatory pathway (Borovikova et al., 2000; Pavlov and Tracey, 2005). Due to the chronic attenuation of HPC cholinergic tone observed in CAF rats, and given that a WD has been shown to provoke a pro-inflammatory response with unknown long-term impacts (Jena et al., 2018; Sobesky et al., 2014), we next examined protein levels of the pro-inflammatory cytokines TNF-α, IL-6, and IL-1β through Western blotting in the dorsal HPC in CAF and CTL rats after the healthy diet intervention period. Results revealed no differences in the levels of any of these markers (Fig. S7).

3.6. Early life WD disrupts acute ACh signaling dynamics during memory testing

Given that early life WD consumption resulted in enduring memory dysfunction and decreases in HPC ACh tone, we next investigated whether acute ACh signaling dynamics during the contextual episodic memory task were altered in CAF vs. CTL rats. After the 30-day healthy diet intervention period, CAF and CTL animals underwent the NOIC behavioral task with simultaneous recording of ACh signaling via *in vivo* fiber photometry (Fig. 5A and B). Replicating the results from our previous cohorts, results revealed that CAF rats were impaired in the task (Fig. 5C). CTL rats showed increased ACh release at the moment of investigating the object novel to the context compared to the object familiar to the context on the test day (day 3; Fig. 5D, Fig. S8), whereas CAF rats showed no difference in ACh release upon investigating the two objects on the test day (Fig. 5E, Fig. S8). Comparing between groups, the extent of ACh release at the onset of exploring the object novel to the context was significantly elevated in CTL rats compared to CAF rats (Fig. 5F), but there were no differences in ACh release between groups at

the onset of investigating the object familiar to the context (Fig. 5G). Additionally, there were no differences in ACh release when investigating the objects upon initial exposure to them on NOIC day 1 (Fig. S8). Collectively, these findings reveal early life WD access has lasting effects on the temporal dynamics of ACh signaling in the HPC during discrimination of a context-object novelty.

To determine whether these ACh release photometric data were related to memory performance, we regressed the extent of HPC DGd ACh release with memory performance (shift from baseline in the NOIC task) with both CAF and CTL groups combined and observed a strong positive correlation, such that the better the rats did in the memory task, the greater the ACh release during object-contextual novelty encounter (Fig. 5H). When separated by diet group, the positive correlation remained for the CTL group of rats (Fig. 5I) but dissipated for the CAF group (Fig. 5J). These results indicate that in CTL rats, with intact ACh neurotransmission, better memory performance was linked with increased ACh signaling upon object-context novelty encounter, whereas no such link was found in CAF rats with disrupted ACh neurotransmission.

### 3.7. ACh agonists reverse early life WD-induced memory impairments

Given the long-term reduction in HPC ACh tone and altered temporal HPC ACh dynamics in CAF rats, we next sought to determine whether pharmacological administration of ACh receptor agonists could rescue the long-lasting deficits in memory function in CAF rats. On day 2 of the HPC-dependent NOIC task (tested after a healthy diet intervention), each rat was given bilateral infusions of either a general ACh receptor agonist (AChRa; carbachol), an α7 nicotinic receptor ACh agonist (α7nAChRa; PNU 282987), or vehicle 3–8 min immediately prior to undergoing the task (Fig. 6A and B). On the subsequent test day of the task, rats that received either AChRa (carbachol) or α7nAChRa (PNU) exhibited improved memory performance compared to rats receiving vehicle alone, with the latter group showing memory performance at chance levels analogous CAF rats in preceding experiments (Fig. 6C). These findings not only reveal that early life WD-induced memory impairments are reversed by augmenting ACh transmission during the encoding and consolidation phases of the memory task, but also that α7 nicotinic receptor signaling likely underlies the WD-induced memory dysfunction.
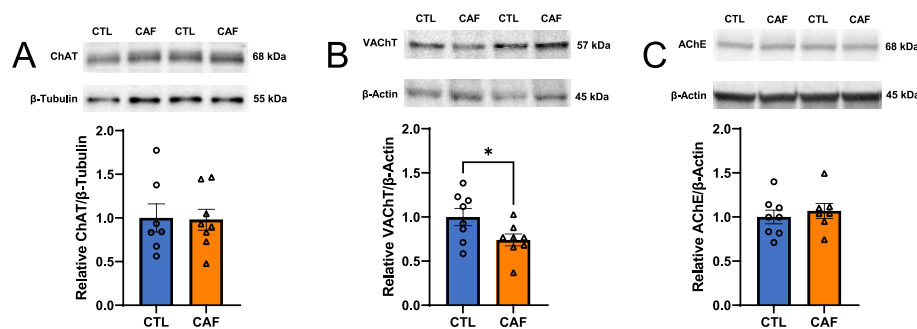
Fig. 4. Early life Western diet (WD) leads to long-lasting reduction in hippocampal cholinergic tone. (A) Immunoblot representative images and results for choline acetyltransferase (ChAT) protein levels in the dorsal hippocampus (HPC) of rats following WD access in early life and a healthy diet intervention in adulthood (N = 15 total, n = 7 CTL due to outlier, n = 8 CAF; unpaired *t*-test [2-tailed], P = 0.9165). (B) Immunoblot representative images and results for vesicular acetylcholine transporter (VAChT) protein levels in the dorsal HPC of rats following early life WD access and a healthy diet intervention in adulthood (N = 16 total, n = 8 CTL, n = 8 CAF; unpaired *t*-test [2-tailed], P = 0. 0449). (C) Immunoblot representative images and results for acetylcholinesterase (AChE) protein levels in the dorsal HPC of rats following WD access in early life and a healthy diet intervention in adulthood (N = 15 total, n = 8 CTL, n = 7 CAF due to outlier; unpaired *t*-test [2-tailed], P = 0. 5570). ACh, acetylcholine; AChE, acetylcholinesterase; CAF, cafeteria diet group; ChAT, choline acetyltransferase; CTL, control group; HPC, hippocampus; VAChT, vesicular acetylcholine transporter; WD, Western diet. Error bars represent ± SEM. *P < 0.05.
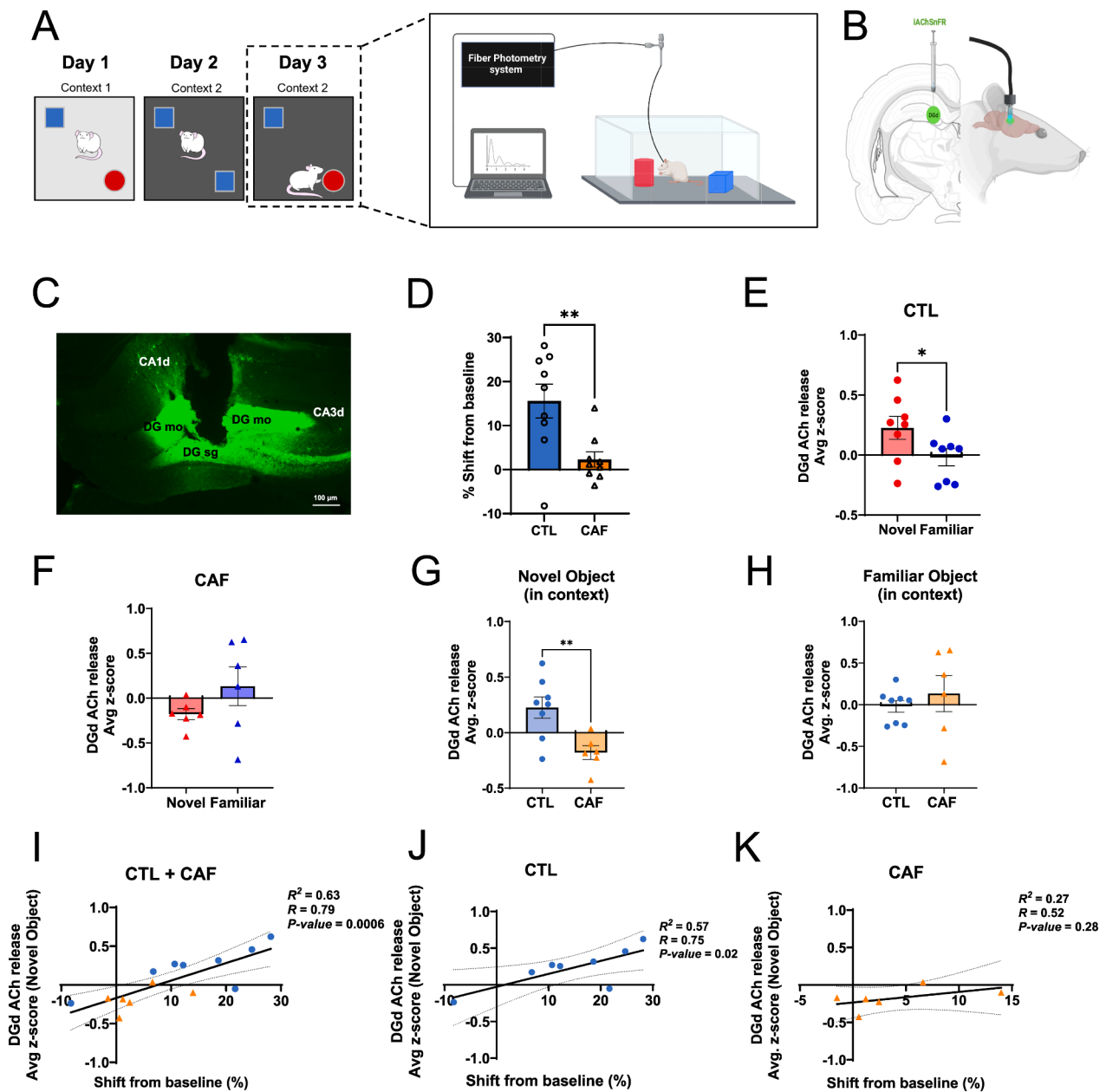
Fig. 5. Early life Western diet (WD) disrupts hippocampal cholinergic release upon contextual-object novelty encounter during episodic memory testing. (A) Behavioral scheme for the Novel Object in Context contextual episodic memory task coupled with *in vivo* fiber photometry. (B) *In vivo* fiber photometry approach to track acetylcholine (ACh) release in the dentate gyrus (DG) region of the dorsal hippocampus (HPC). (C) Representative photomicrograph of iAChSnFR viral expression and cannula placement in the dorsal DG of the HPC. (D) NOIC percent shift from baseline performance following healthy diet intervention and with implementation of *in vivo* fiber photometry (N = 18 total, n = 9 CTL, n = 9 CAF; unpaired *t*-test [2-tailed]; P = 0.0064). (E) Average z-score of ACh release in the DG at the onset of exploring the novel vs. familiar objects during the test day of NOIC in CTL rats (N = 8 total, n = 8 CTL group only, paired *t*-test [2-tailed], P = 0.0140; two-way ANOVA (diet, object [as repeated measure], diet × object interaction), P = 0.0087 for diet × object interaction). (F) Average z-score of ACh release in the DG at the onset of exploring the novel vs. familiar objects during the test day of NOIC in CAF rats (N = 6 total, n = 6 CAF group only, paired *t*-test [2-tailed], P = 0.1453; two-way ANOVA (diet, object [as repeated measure], diet × object interaction), P = 0.0087 for diet × object interaction). (G) Comparison of average z-score of ACh release in the DG at the onset of exploring the novel object during the test day of NOIC in CTL vs. CAF rats (N = 14 total, n = 8 CTL, n = 6 CAF; unpaired *t*-test [2-tailed], P = 0.0068; two-way ANOVA (diet, object [as repeated measure], diet × object interaction), P = 0.0087 for diet × object interaction and P = 0.0478 for novel object comparison between diet groups). (H) Comparison of average z-score of ACh release in the DG at the onset of exploring the familiar object during the test day of NOIC in CTL vs. CAF rats (N = 14 total, n = 8 CTL, n = 6 CAF; unpaired *t*-test [2-tailed], P = 0.4641; two-way ANOVA (diet, object [as repeated measure], diet × object interaction), P = 0.0087 for diet × object interaction and P = 0.6038 for familiar object comparison between diet groups). (I) Regression of average z-score of ACh release at the onset of novel object exploration on percent shift from baseline NOIC memory performance (N = 14 total, n = 8 CTL, n = 6 CAF; R^2 = 0.63, P = 0.0006). (J) Regression of average z-score of ACh release at the onset of novel object exploration on percent shift from baseline NOIC memory performance in CTL rats only (N = 8 total, n = 8 CTL; R^2 = 0.57, P = 0.02). (K) Regression of average z-score of ACh release at the onset of novel object exploration on percent shift from baseline NOIC memory performance in CAF rats only (N = 6 total, n = 6 CAF; R^2 = 0.27, P = 0.28). ACh, acetylcholine; CA1d, dorsal CA1 subregion of the hippocampus; CA3d, dorsal CA3 subregion of the hippocampus; CAF, cafeteria diet group; CTL, control group; DG, dentate gyrus; DG mo, molecular layer of the dentate gyrus; DG sg, subgranular layer of the dentate gyrus; HPC, hippocampus; NOIC, Novel Object in Context; WD, Western diet. Error bars represent ± SEM. *P < 0.05, **P < 0.01.
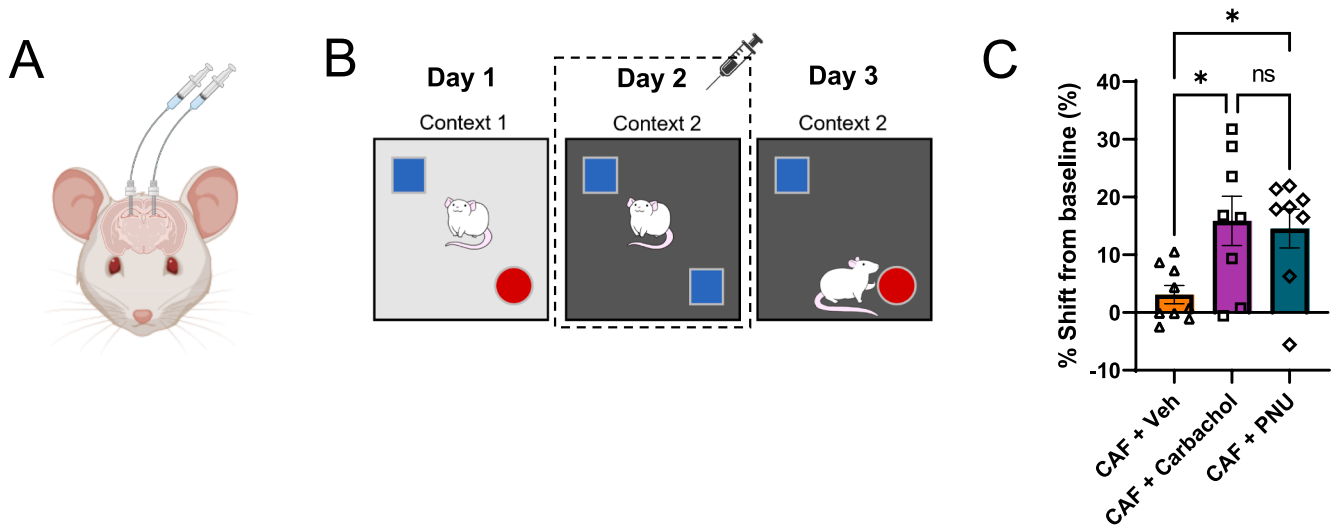
Fig. 6. Pharmacological administration of acetylcholine agonists improves Western diet-induced memory performance. (A) Illustration of bilateral indwelling catheter infusions into the dorsal HPC. (B) Schematic of the Novel Object in Context (NOIC) contextual episodic memory task depicting timing of acetylcholine (ACh) agonist infusion on day 2. (C) NOIC percent shift from baseline performance following healthy diet intervention and with ACh infusion on day 2 (N = 25 total, n = 9 CAF + Vehicle, n = 8 CAF + Carbachol [general ACh agonist], n = 8 CAF + PNU [α7 nicotinic receptor agonist] due to outliers; One-way ANOVA (infusion group) with Tukey's post-hoc test for multiple comparisons; $F_{(2,22)} = 5.122$ and $P = 0.0149$ for overall model, for multiple comparisons: CAF + Vehicle vs. CAF + Carbachol: $P = 0.0226$ with n = 22 degrees of freedom (df), CAF + Vehicle vs. CAF + PNU: $P = 0.0431$ with n = 22 df, CAF + Carbachol vs. CAF + PNU: $P = 0.9542$ with n = 22 df). ACh, acetylcholine; CAF, cafeteria diet group; CTL, control group; HPC, hippocampus; NOIC, Novel Object in Context; WD, Western diet. Error bars represent $\pm$ SEM. *$P < 0.05$.

4. Discussion

Although the negative metabolic impacts of consuming a Western diet (WD) high in refined sugar, saturated fat, and processed foods have been widely investigated (Heinonen et al., 2014; Luo et al., 2016; Shively et al., 2019; Wilson et al., 2007), much less is known regarding the mechanisms through which WD leads to cognitive impairment. Here we developed an early life rodent WD model that, absent of metabolic or general behavioral abnormalities, yields enduring memory deficits that persist even after healthy diet intervention at the onset of adulthood. Results reveal that these long-lasting early life WD-induced memory impairments are mediated by compromised hippocampus (HPC) acetylcholine (ACh) signaling, manifested both in terms of chronic reductions in HPC ACh tone as well as aberrant acute temporal ACh release dynamics in the HPC during mnemonic evaluation. The translational relevance of these findings is enhanced by additional results revealing that HPC administration of an ACh agonist targeting α7nAChRs during the memory encoding and consolidation phases reversed the WD-induced memory impairments, thus identifying potential pharmacological targets for diet-induced cognitive impairment. While perturbations in the gut microbiome were observed during the early life WD-access period, these outcomes are unlikely to be tied to the memory deficits, as healthy diet intervention in adulthood reversed the microbiome changes but failed to rescue the memory impairments. Collectively, these findings denote a mechanistic role of ACh signaling, and not the gut microbiome, in persistent memory impairments due to WD consumption during early life periods of development.

The reliance of the HPC on ACh for proper memory function and the connection between impaired ACh neurotransmission and Alzheimer's disease (AD) have been well-established (Fadda et al., 1996; Haam and Yakel, 2017; Hasselmo, 2006; Liu et al., 2022; Ma and Qian, 2019). The current findings identify altered ACh signaling as a functional mediator of early life WD-induced alterations in memory function. Previous evidence in adult rats receiving either a WD containing 22 % kcal from fat, a high-fat diet containing 60 % kcal from fat, or a control diet containing 7 % kcal from fat for 12 weeks showed no differences in levels of ChAT in

the medial septum/vertical limb of the diagonal band or in levels of AChE in the HPC despite impairments in spatial memory for the WD and high-fat diet groups (Kosari et al., 2012). Integrated with our present results, this suggests early life (juvenile-adolescence) is a critical period for dietary exposure to impact HPC ACh neuronal pathway development. This is further supported by previous research indicating that administration of choline (an ACh precursor) throughout gestation and up through PN 24 enhanced spatial memory of rats in adulthood (Meck et al., 1988). In contrast, a recent study in diet-induced obese adult rats revealed increased levels of ChAT in the HPC after 5 and 17 weeks' consumption of a high-fat diet containing 45 % kcal from fat, decreased levels of AChE in the HPC after 17-week consumption of the diet, and increased level of VAChT in the HPC after 17-week consumption of the diet compared to control chow-fed rats (Martinelli et al., 2022). Furthermore, expression of the α7nAChR (nicotinic) was decreased at both 5 and 17 weeks on the diet in the HPC, while no effects were observed for muscarinic ACh receptor subtypes 1, 3, or 5 in the HPC regardless of time point (Martinelli et al., 2022). With the exception of the decreased level of α7nAChR, these findings suggest that ACh neurotransmission was increased in animals fed a high-fat diet, yet an important factor for consideration is that no behavior tests were performed to assess HPC function or other cognitive tasks. In addition, the study design differed in age of the rats and the duration of diet exposure compared to our present work. However, this previous study did identify that α7nAChR is more susceptible to high-fat dietary insults, which aligns with our current finding that selective agonism of α7nAChR rescued early life WD-induced HPC memory impairments.

Given this connection between diet, memory, and ACh signaling, an imperative topic of future research is to specifically determine how diet is ultimately giving rise to altered ACh neurotransmission and, furthermore, whether this leads to a predisposition to develop AD or other forms of dementia. We hypothesize a role for gastrointestinal (GI)-originating vagus nerve signaling in mediating WD-associated alterations in HPC ACh signaling. For example, we recently demonstrated that ablation of GI-specific vagal sensory signaling impairs HPC-dependent contextual episodic memory in rats (Suarez et al., 2018). In

this report we also identified the medial septum as an anatomical relay connecting vagal signaling to the dorsal HPC. Given that the medial septum is a principal source of ACh input to the HPC, it may be that blunted GI-derived vagal signaling contributes to the altered ACh signaling associated with early life WD. While additional work is required to support this hypothesis, it is the case that WD consumption is associated with blunted GI vagal signaling (Covasa et al., 2000; de Lartigue et al., 2012; Savastano and Covasa, 2005), thus providing additional evidence for this working model (Suarez et al., 2018).

While we did not observe elevated levels of pro-inflammatory cytokines in the dorsal HPC after the healthy diet intervention, previous research has identified a cholinergic anti-inflammatory pathway in which α7nAChR activation plays a pivotal role (Borovikova et al., 2000; Patel et al., 2017; Pavlov and Tracey, 2005; Shytle et al., 2004; Wang et al., 2003). In light of previous evidence indicating that early life HFCS consumption increased levels of pro-inflammatory cytokines in the dorsal HPC (Hsu et al., 2015), it is possible that neuroinflammation was present during the early life WD consumption period in the current study and then reversed upon the healthy diet intervention. Given existing evidence for pro-inflammatory effects of a WD (Jena et al., 2018; Sobesky et al., 2014), future research is warranted to more thoroughly probe potential connections between WD consumption during early life, neuroinflammation, and ACh neurotransmission.

Our results clearly show that consumption of WD in early life markedly altered the gut microbiome, but, when the animals were switched to a healthy diet in adulthood, the alterations were largely reversed. The initial changes in the gut microbiome between CAF and CTL rats were expected, considering that the diets for each group were very distinct with marked differences in dietary fiber content, dietary fiber type (e.g., source, structure), macronutrient composition, micronutrient characteristics, and energy density, among other factors, which have been linked with shifts in gut microbial taxonomic populations in both humans and animal studies (Baxter et al., 2019; de La Serre et al., 2010; Fava et al., 2013; Tap et al., 2015). However, persistence of diet-induced taxonomic shifts in the gut microbiome have varied by age of exposure to a given diet, duration of diet exposure, type of diet used, host genome, and sex, among a variety of other potential factors (Ericsson and Franklin, 2021; Franklin and Ericsson, 2017). In our previous work with the same early life CAF diet model implemented in females, gut microbiome differences following the healthy diet intervention became more disparate (Tsan et al., 2022b) instead of being reversed as with the current study in males. Previous research has shown that male and female mice have distinctly different bacterial taxonomic compositions as well as bacterial diversity in adulthood, independent of diet (Unger et al., 2019; Zhang et al., 2020). Given that the machine learning analyses in the present study indicate that early WD-associated microbiome changes were not associated with long- (after dietary intervention) term memory impairments in males, and also that males and females display divergent WD-induced gut microbiome phenotypes in adulthood yet both have long-lasting HPC-dependent cognitive deficits (Tsan et al., 2022b), we conclude that the gut microbiome is unlikely to be mediating the enduring HPC dysfunction associated with early life WD. To further support this and lend evidence that the microbiome is not related to altered HPC ACh neurotransmission, our correlational analyses between microbial taxa and HPC VAChT levels in male rats revealed no significant relationships, and the five bacterial taxa that differed in abundance between groups after the healthy diet intervention period were not significantly correlated with memory performance either before or after the healthy diet intervention. Regardless, whether aberrant HPC ACh signaling is functionally connected to WD-associated memory impairments in females requires further experimentation to fully elucidate.

An important distinction of the current findings is that the persistent WD-induced memory impairments due to altered ACh signaling occurred in the absence of effects on metabolic outcomes and body weight. This signifies that early life diet can have a critical, long-lasting

effects on neural function – independently of obesity. Previous research has also found HPC-dependent memory impairments in the absence of differences in body weight or metabolic markers following early life free-access to 11 % sugar or 11 % HFCS in rats (Noble et al., 2019), or before the onset of body weight differences in mice or rats fed a high-fat diet (Kaczmarczyk et al., 2013; Kanoski and Davidson, 2010). These findings suggest that development of HPC-dependent neurocognitive deficits may precede weight gain and an obesity phenotype. However, in the present study the CAF rats were hyperphagic compared to controls during the CAF exposure period. One possibility for this caloric intake-body weight mismatch is based on a micronutrient deficiency in the CAF group. This is unlikely, however, as the predominant source of calories in the CAF model was the commercially-available high-fat diet, which provides sufficient micronutrient access. A more likely explanation is that the CAF model altered energy expenditure. Consistent with this notion, previous research has shown that consumption of palatable cafeteria-style WDs increase energy expenditure in rodents, even in the absence of a running wheel or other forms of exercise (Bjursell et al., 2008; El Ayadi et al., 2021; Rothwell and Stock, 1982). However, putative changes in energy expenditure are unlikely to account for the HPC dysfunction given that there was no caloric intake-body weight mismatch when memory impairments were observed after the healthy dietary intervention. Although no differences in body weight were observed in the present work, we reason that challenging rats with our WD in adulthood would likely have caused an obesity phenotype, especially given existing evidence indicating that impairments in HPC dependent memory predict weight gain when rats consume a high-fat diet (Davidson et al., 2009; Davidson et al., 2013).

The present study has some limitations to be considered. Accurately measuring caloric intake in individual animals necessitated the methodological decision to singly house rats, but this could also have altered the vulnerability of the HPC to dietary insults or other stressors. Although in the present work WD-induced memory impairments persisted despite a healthy diet intervention in adulthood, some previous studies have found that a standard/healthy diet intervention rescues memory deficits in other WD models (Boitard et al., 2016; Hao et al., 2016; Nicolas et al., 2022; Sobesky et al., 2014; Tran and Westbrook, 2017). Differences in type of WD (e.g., types of foods, macronutrient profiles), duration of exposure to a given WD and standard/healthy diet, and age during exposure could be related to the discrepant findings. Accordingly, the CAF diet we used to model a WD does not allow for determination of which specific dietary component(s) or macronutrient (s) give rise to the effects observed. We also did not directly investigate a role for sex and/or sex hormones. Given that our previous work in female rats showed early life WD-access led to initial deviations in the gut microbiome that became more apparent after the healthy diet intervention (vs. controls) – an effect not observed in males – it is possible that early life WD exposure has sex-specific effects. Further, while we did not determine whether cholinergic agonism alters performance in the NOIC memory task in control animals never exposed to the WD, it is important to note that HPC ACh signaling exhibits an inverted U-shape in function (Geerts, 2012; Karami et al., 2021) and thus we hypothesize that ACh agonism in healthy control rats may actually compromise their memory performance. Finally, as is inherent with all animal models, the translation to humans is nonlinear. However, it should be underscored that WD consumption is also linked with memory impairments and elevated AD risk in humans (Sullivan, 2020; Wieckowska-Gacek et al., 2021). Given that AD is associated with aberrant HPC ACh signaling, the present results may provide important translational insight into links between the early life dietary environment and late-life neurocognitive impairments. In light of previous evidence identifying a cholinergic anti-inflammatory pathway involving α7nAChR activation in glial cells, astrocytes, and vascular mural cells (Li et al., 2019; Shytle et al., 2004; Wang et al., 2003), future research is needed to examine the connections between vasodynamics, cholinergic signaling, and cognitive impairments in distinct cell types. Although we used ACh agonists that were

not selective for a specific cell type, α7nAChR is more highly expressed in neurons than other cell types and the ACh sensor used in fiber photometry was expressed via a neuron-specific promoter (Borden et al., 2020; Chen et al., 2021; Dani and Bertrand, 2007; Zhu et al., 2020), collectively lending support for the hypothesis that neural cells played a larger role than other cell types in the observed cognitive impairments.

The present findings collectively reveal a mechanistic connection between early life exposure to a WD, long-lasting contextual episodic memory impairments, and ACh neurotransmission. The α7 nicotinic receptor was found to be a key intermediary of the WD-induced disrupted memory function, and persistent memory deficits were observed independent of altered metabolic outcomes or general behavior abnormalities – and were not specifically linked to alterations in the gut microbiome. Overall, this work identifies a link between early life diet and impaired ACh neurotransmission in the HPC. Whether these findings have translational relevance to the etiology of human dementia warrants further investigation.

CRediT authorship contribution statement

Anna M.R. Hayes: Conceptualization, Data curation, Formal analysis, Investigation, Methodology, Visualization, Writing – original draft, Writing – review & editing. **Logan Tierno Lauer:** Formal analysis, Investigation. **Alicia E. Kao:** Investigation. **Shan Sun:** Formal analysis, Visualization. **Molly E. Klug:** Investigation. **Linda Tsan:** Conceptualization, Investigation. **Jessica J. Rea:** Investigation. **Keshav S. Subramanian:** Investigation. **Cindy Gu:** Investigation. **Natalie Tanios:** Investigation. **Arun Ahuja:** Investigation. **Kristen N. Donohue:** Investigation, Methodology. **Léa Décarie-Spain:** Investigation, Methodology. **Anthony A. Fodor:** Formal analysis, Visualization. **Scott E. Kanoski:** Conceptualization, Formal analysis, Funding acquisition, Methodology, Resources, Supervision, Visualization, Writing – review & editing.

Declaration of competing interest

The authors declare that they have no known competing financial interests or personal relationships that could have appeared to influence the work reported in this paper.

Data availability

Data will be made available on request.

Acknowledgements

Funding

Declaration of interest

The authors declare no conflicts of interest. This manuscript has been posted as a preprint on bioRxiv (https://doi.org/10.1101/2023.07.21. 550120).

Data statement

The data that support the findings of this study are available from the corresponding author, S.E.K., upon reasonable request.

Appendix A. Supplementary data

Supplementary data to this article can be found online at https://doi.org/10.1016/j.bbi.2024.03.015.

References

Albasser, M.M., Amin, E., Iordanova, M.D., Brown, M.W., Pearce, J.M., Aggleton, J.P., 2011. Perirhinal cortex lesions uncover subsidiary systems in the rat for the detection of novel and familiar objects. Eur. J. Neurosci. 34, 331–342.

André, C., Dinel, A.-L., Ferreira, G., Layé, S., Castanon, N., 2014. Diet-induced obesity progressively alters cognition, anxiety-like behavior and lipopolysaccharide-induced depressive-like behavior: focus on brain indoleamine 2,3-dioxygenase activation. Brain Behav. Immun. 41, 10–21.

Balderas, I., Rodriguez-Ortiz, C.J., Salgado-Tonda, P., Chavez-Hurtado, J., McGaugh, J. L., Bermudez-Rattoni, F., 2008. The consolidation of object and context recognition memory involve different regions of the temporal lobe. Learn. Mem. 15, 618–624.

Baxter, N.T., Schmidt, A.W., Venkataraman, A., Kim, K.S., Waldron, C., Schmidt, T.M., 2019. Dynamics of human gut microbiota and short-chain fatty acids in response to dietary interventions with three fermentable fibers. MBio 10, e02566–02518.

Baym, C.L., Khan, N.A., Monti, J.M., Raine, L.B., Drollette, E.S., Moore, R.D., Scudder, M. R., Kramer, A.F., Hillman, C.H., Cohen, N.J., 2014. Dietary lipids are differentially associated with hippocampal-dependent relational memory in prepubescent children1,2,3,4. Am. J. Clin. Nutr. 99, 1026–1033.

Bird, C.M., Burgess, N., 2008. The hippocampus and memory: insights from spatial processing. Nat. Rev. Neurosci. 9, 182–194.

Bjursell, M., Gerdin, A.-K., Lelliott, C.J., Egecioglu, E., Elmgren, A., Törnell, J., Oscarsson, J., Bohlooly-Y, M., 2008. Acutely reduced locomotor activity is a major contributor to Western diet-induced obesity in mice. Am. J. Physiol.-Endocrinol. Metabolism 294, E251–E260.

Boitard, C., Parkes, S.L., Cavaroc, A., Tantot, F., Castanon, N., Layé, S., Tronel, S., Pacheco-Lopez, G., Coutureau, E., Ferreira, G., 2016. Switching adolescent high-fat diet to adult control diet restores neurocognitive alterations. Front. Behav. Neurosci. 10.

Borden, P.M., Zhang, P., Shivange, A.V., Marvin, J.S., Cichon, J., Dan, C., Podgorski, K., Figueiredo, A., Novak, O., Tanimoto, M., Shigetomi, E., Lobas, M.A., Kim, H., Zhu, P. K., Zhang, Y., Zheng, W.S., Fan, C., Wang, G., Xiang, B., Gan, L., Zhang, G.-X., Guo, K., Lin, L., Cai, Y., Yee, A.G., Aggarwal, A., Ford, C.P., Rees, D.C., Dietrich, D., Khakh, B.S., Dittman, J.S., Gan, W.-B., Koyama, M., Jayaraman, V., Cheer, J.F., Lester, H.A., Zhu, J.J., Looger, L.L., 2020. A fast genetically encoded fluorescent sensor for faithful <i>in vivo</i> acetylcholine detection in mice, fish, worms and flies. Cold Spring Harbor Laboratory.

Borovikova, L.V., Ivanova, S., Zhang, M., Yang, H., Botchkina, G.I., Watkins, L.R., Wang, H., Abumrad, N., Eaton, J.W., Tracey, K.J., 2000. Vagus nerve stimulation attenuates the systemic inflammatory response to endotoxin. Nature 405, 458–462.

Broadbent, N.J., Squire, L.R., Clark, R.E., 2004. Spatial memory, recognition memory, and the hippocampus. Proc. Natl. Acad. Sci. 101, 14515–14520.

Bunce, J.G., Sabolek, H.R., Chrobak, J.J., 2004. Intraseptal infusion of the cholinergic agonist carbachol impairs delayed-non-match-to-sample radial arm maze performance in the rat. Hippocampus 14, 450–459.

Caine, S.B., Geyer, M.A., Swerdlow, N.R., 1991. Carbachol infusion into the dentate gyrus disrupts sensorimotor gating of startle in the rat. Psychopharmacology 105, 347–354.

Carlini, V.P., Ghersi, M., Gabach, L., Schiöth, H.B., Pérez, M.F., Ramirez, O.A., Fiol de Cuneo, M., de Barioglio, S.R., 2011. Hippocampal effects of neuronostatin on memory, anxiety-like behavior and food intake in rats. Neuroscience 197, 145–152.

Chen, J., Cho, K.E., Skwarzynska, D., Clancy, S., Conley, N.J., Clinton, S.M., Li, X., Lin, L., Zhu, J.J., 2021. The property-based practical applications and solutions of genetically encoded acetylcholine and monoamine sensors. J. Neurosci. 41, 2318–2328.

Clark, K.A., Alves, J.M., Jones, S., Yunker, A.G., Luo, S., Cabeen, R.P., Angelo, B., Xiang, A.H., Page, K.A., 2020. Dietary fructose intake and hippocampal structure and connectivity during childhood. Nutrients 12, 909.

Clark, R.E., Broadbent, N.J., Squire, L.R., 2005. Hippocampus and remote spatial memory in rats. Hippocampus 15, 260–272.

Cohen, S.J., Stackman Jr, R.W., 2015. Assessing rodent hippocampal involvement in the novel object recognition task. A review. Behav. Brain Res. 285, 105–117.

Covasa, M., Grahn, J., Ritter, R.C., 2000. High fat maintenance diet attenuates hindbrain neuronal response to CCK. Regul. Pept. 86, 83–88.

Dani, J.A., Bertrand, D., 2007. Nicotinic acetylcholine receptors and nicotinic cholinergic mechanisms of the central nervous system. Annu. Rev. Pharmacol. Toxicol. 47, 699–729.

David, L.A., Maurice, C.F., Carmody, R.N., Gootenberg, D.B., Button, J.E., Wolfe, B.E., Ling, A.V., Devlin, A.S., Varma, Y., Fischbach, M.A., 2014. Diet rapidly and reproducibly alters the human gut microbiome. Nature 505, 559–563.

Davidson, T.L., Chan, K., Jarrard, L.E., Kanoski, S.E., Clegg, D.J., Benoit, S.C., 2009. Contributions of the hippocampus and medial prefrontal cortex to energy and body weight regulation. Hippocampus 19, 235–252.

Davidson, T.L., Monnot, A., Neal, A.U., Martin, A.A., Horton, J.J., Zheng, W., 2012. The effects of a high-energy diet on hippocampal-dependent discrimination performance and blood–brain barrier integrity differ for diet-induced obese and diet-resistant rats. Physiol. Behav. 107, 26–33.

Davidson, T.L., Hargrave, S.L., Swithers, S.E., Sample, C.H., Fu, X., Kinzig, K.P., Zheng, W., 2013. Inter-relationships among diet, obesity and hippocampal-dependent cognitive function. Neuroscience 253, 110–122.

Davis, E.A., Wald, H.S., Suarez, A.N., Zubcevic, J., Liu, C.M., Cortella, A.M., Kamitakahara, A.K., Polson, J.W., Arnold, M., Grill, H.J., De Lartigue, G., Kanoski, S. E., 2020. Ghrelin signaling affects feeding behavior, metabolism, and memory through the vagus nerve. Curr. Biol. 30, 4510–4518.e4516.

De Filippo, C., Cavalieri, D., Di Paola, M., Ramazzotti, M., Poullet, J.B., Massart, S., Collini, S., Pieraccini, G., Lionetti, P., 2010. Impact of diet in shaping gut microbiota revealed by a comparative study in children from Europe and rural Africa. Proc. Natl. Acad. Sci. 107, 14691–14696.

de La Serre, C.B., Ellis, C.L., Lee, J., Hartman, A.L., Rutledge, J.C., Raybould, H.E., 2010. Propensity to high-fat diet-induced obesity in rats is associated with changes in the gut microbiota and gut inflammation. Am. J. Physiol. 299, G440–G448.

de Lartigue, G., Barbier de la Serre, C., Espero, E., Lee, J., Raybould, H.E., 2012. Leptin resistance in vagal afferent neurons inhibits cholecystokinin signaling and satiation in diet induced obese rats. PLoS One 7, e32967.

Décarie-Spain, L., Liu, C.M., Lauer, L.T., Subramanian, K., Bashaw, A.G., Klug, M.E., Gianatiempo, I.H., Suarez, A.N., Noble, E.E., Donohue, K.N., Cortella, A.M., Hahn, J. D., Davis, E.A., Kanoski, S.E., 2022. Ventral hippocampus-lateral septum circuitry promotes foraging-related memory. Cell Rep. 40, 111402.

Dunbar, G.L., Rylett, R.J., Schmidt, B.M., Sinclair, R.C., Williams, L.R., 1993. Hippocampal choline acetyltransferase activity correlates with spatial learning in aged rats. Brain Res. 604, 266–272.

El Ayadi, A., Tapking, C., Prasai, A., Rontoyanni, V.G., Abdelrahman, D.R., Cui, W., Fang, G., Bhattarai, N., Murton, A.J., 2021. Cafeteria diet impacts the body weight and energy expenditure of Brown Norway rats in an apparent age dependent manner, but has no effect on muscle anabolic sensitivity to nutrition. Front. Nutr. 8, 719612.

Ericsson, A.C., Franklin, C.L., 2021. The gut microbiome of laboratory mice: considerations and best practices for translational research. Mamm. Genome 32, 239–250.

Fadda, F., Melis, F., Stancampiano, R., 1996. Increased hippocampal acetylcholine release during a working memory task. Eur. J. Pharmacol. 307, R1–R2.

Fava, F., Gitau, R., Griffin, B.A., Gibson, G., Tuohy, K., Lovegrove, J., 2013. The type and quantity of dietary fat and carbohydrate alter faecal microbiome and short-chain fatty acid excretion in a metabolic syndrome 'at-risk'population. Int. J. Obes. (Lond) 37, 216–223.

Ferreira, A., Castro, J.P., Andrade, J.P., Dulce Madeira, M., Cardoso, A., 2018. Cafeteria-diet effects on cognitive functions, anxiety, fear response and neurogenesis in the juvenile rat. Neurobiol. Learn. Mem. 155, 197–207.

Francis, H., Stevenson, R., 2013. The longer-term impacts of Western diet on human cognition and the brain. Appetite 63, 119–128.

Franklin, C.L., Ericsson, A.C., 2017. Microbiota and reproducibility of rodent models. Lab Anim. 46, 114–122.

Geerts, H., 2012. α7 nicotinic receptor modulators for cognitive deficits in schizophrenia and Alzheimer's disease. Expert Opin. Invest. Drugs 21, 59–65.

Guo, Y., Zhu, X., Zeng, M., Qi, L., Tang, X., Wang, D., Zhang, M., Xie, Y., Li, H., Yang, X., Chen, D., 2021. A diet high in sugar and fat influences neurotransmitter metabolism and then affects brain function by altering the gut microbiota. Transl. Psychiatry 11, 328.

Haam, J., Yakel, J.L., 2017. Cholinergic modulation of the hippocampal region and memory function. J. Neurochem. 142, 111–121.

Haider, S., Saleem, S., Perveen, T., Tabassum, S., Batool, Z., Sadir, S., Liaquat, L., Madiha, S., 2014. Age-related learning and memory deficits in rats: role of altered brain neurotransmitters, acetylcholinesterase activity and changes in antioxidant defense system. Age 36.

Hao, S., Dey, A., Yu, X., Stranahan, A.M., 2016. Dietary obesity reversibly induces synaptic stripping by microglia and impairs hippocampal plasticity. Brain Behav. Immun. 51, 230–239.

Hasselmo, M.E., 2006. The role of acetylcholine in learning and memory. Curr. Opin. Neurobiol. 16, 710–715.

Heinonen, I., Rinne, P., Ruohonen, S.T., Ruohonen, S., Ahotupa, M., Savontaus, E., 2014. The effects of equal caloric high fat and western diet on metabolic syndrome, oxidative stress and vascular endothelial function in mice. Acta Physiol. 211, 515–527.

Henke, K., Weber, B., Kneifel, S., Wieser, H.G., Buck, A., 1999. Human hippocampus associates information in memory. Proc. Natl. Acad. Sci.96, 5884–5889.

Hsu, T.M., Konanur, V.R., Taing, L., Usui, R., Kayser, B.D., Goran, M.I., Kanoski, S.E., 2015. Effects of sucrose and high fructose corn syrup consumption on spatial memory function and hippocampal neuroinflammation in adolescent rats. Hippocampus 25, 227–239.

Jarrard, L.E., 1993. On the role of the hippocampus in learning and memory in the rat. Behav. Neural Biol. 60, 9–26.

Jena, P.K., Sheng, L., Di Lucente, J., Jin, L.W., Maezawa, I., Wan, Y.J.Y., 2018. Dysregulated bile acid synthesis and dysbiosis are implicated in Western diet–induced systemic inflammation, microglial activation, and reduced neuroplasticity. FASEB J. 32, 2866–2877.

Kaczmarczyk, M.M., Machaj, A.S., Chiu, G.S., Lawson, M.A., Gainey, S.J., York, J.M., Meling, D.D., Martin, S.A., Kwakwa, K.A., Newman, A.F., Woods, J.A., Kelley, K.W., Wang, Y., Miller, M.J., Freund, G.G., 2013. Methylphenidate prevents high-fat diet (HFD)-induced learning/memory impairment in juvenile mice. Psychoneuroendocrinology 38, 1553–1564.

Kanoski, S.E., 2012. Cognitive and neuronal systems underlying obesity. Physiol. Behav. 106, 337–344.

Kanoski, S.E., Davidson, T.L., 2010. Different patterns of memory impairments accompany short- and longer-term maintenance on a high-energy diet. J. Exp. Psychol. Anim. Behav. Process. 36, 313–319.

Kanoski, S.E., Davidson, T.L., 2011. Western diet consumption and cognitive impairment: links to hippocampal dysfunction and obesity. Physiol. Behav. 103, 59–68.

Kanoski, S.E., Zhang, Y., Zheng, W., Davidson, T.L., 2010. The effects of a high-energy diet on hippocampal function and blood-brain barrier integrity in the rat. J. Alzheimers Dis. 21, 207–219.

Kanoski, S.E., Fortin, S.M., Ricks, K.M., Grill, H.J., 2013. Ghrelin signaling in the ventral hippocampus stimulates learned and motivational aspects of feeding via PI3K-akt signaling. Biol. Psychiatry 73, 915–923.

Karami, A., Darreh-Shori, T., Schultzberg, M., Eriksdotter, M., 2021. CSF and plasma cholinergic markers in patients with cognitive impairment. Front. Aging Neurosci. 13.

Kendig, M.D., Boakes, R.A., Rooney, K.B., Corbit, L.H., 2013. Chronic restricted access to 10% sucrose solution in adolescent and young adult rats impairs spatial memory and alters sensitivity to outcome devaluation. Physiol. Behav. 120, 164–172.

Kosari, S., Badoer, E., Nguyen, J.C.D., Killcross, A.S., Jenkins, T.A., 2012. Effect of western and high fat diets on memory and cholinergic measures in the rat. Behav. Brain Res. 235, 98–103.

Levin, E.D., McClernon, F.J., Rezvani, A.H., 2006. Nicotinic effects on cognitive function: behavioral characterization, pharmacological specification, and anatomic localization. Psychopharmacology 184, 523–539.

Li, D.-J., Tong, J., Zeng, F.-Y., Guo, M., Li, Y.-H., Wang, H., Wang, P., 2019. Nicotinic ACh receptor α7 inhibits PDGF-induced migration of vascular smooth muscle cells by activating mitochondrial deacetylase sirtuin 3. Br. J. Pharmacol. 176, 4388–4401.

Liu, W., Li, J., Yang, M., Ke, X., Dai, Y., Lin, H., Wang, S., Chen, L., Tao, J., 2022. Chemical genetic activation of the cholinergic basal forebrain hippocampal circuit rescues memory loss in Alzheimer's disease. Alzheimers Res. Ther. 14.

Luo, Y., Burrington, C.M., Graff, E.C., Zhang, J., Judd, R.L., Suksaranjit, P., Kaewpoowat, Q., Davenport, S.K., O'Neill, A.M., Greene, M.W., 2016. Metabolic phenotype and adipose and liver features in a high-fat Western diet-induced mouse model of obesity-linked NAFLD. Am. J. Physiol. 310, E418–E439.

Ma, K.-G., Qian, Y.-H., 2019. Alpha 7 nicotinic acetylcholine receptor and its effects on Alzheimer's disease. Neuropeptides 73, 96–106.

Martinelli, I., Tayebati, S.K., Roy, P., Micioni Di Bonaventura, M.V., Moruzzi, M., Cifani, C., Amenta, F., Tomassoni, D., 2022. Obesity-related brain cholinergic system impairment in high-fat-diet-fed rats. Nutrients 14, 1243.

Martínez, M.C., Villar, M.E., Ballarini, F., Viola, H., 2014. Retroactive interference of object-in-context long-term memory: role of dorsal hippocampus and medial prefrontal cortex. Hippocampus 24, 1482–1492.

Meck, W.H., Smith, R.A., Williams, C.L., 1988. Pre- and postnatal choline supplementation produces long-term facilitation of spatial memory. Dev. Psychobiol. 21, 339–353.

Miller, B.R., Hen, R., 2015. The current state of the neurogenic theory of depression and anxiety. Curr. Opin. Neurobiol. 30, 51–58.

Molteni, R., Wu, A., Vaynman, S., Ying, Z., Barnard, R.J., Gomez-Pinilla, F., 2004. Exercise reverses the harmful effects of consumption of a high-fat diet on synaptic and behavioral plasticity associated to the action of brain-derived neurotrophic factor. Neuroscience 123, 429–440.

Moser, V.A., Pike, C.J., 2017. Obesity Accelerates Alzheimer-Related Pathology in APOE4 but not APOE3 Mice. eNeuro 4.

Nagy, P.M., Aubert, I., 2015. Overexpression of the vesicular acetylcholine transporter enhances dendritic complexity of adult-born hippocampal neurons and improves acquisition of spatial memory during aging. Neurobiol. Aging 36, 1881–1889.

Nicolas, S., Léime, C.S.Ó., Hoban, A.E., Hueston, C.M., Cryan, J.F., Nolan, Y.M., 2022. Enduring effects of an unhealthy diet during adolescence on systemic but not neurobehavioural measures in adult rats. Nutr. Neurosci. 25, 657–669.

Noble, E.E., Hsu, T.M., Jones, R.B., Fodor, A.A., Goran, M.I., Kanoski, S.E., 2017a. Early-life sugar consumption affects the rat microbiome independently of obesity. J. Nutr. 147, 20–28.

Noble, E.E., Hsu, T.M., Kanoski, S.E., 2017b. Gut to brain dysbiosis: mechanisms linking Western diet consumption, the microbiome, and cognitive impairment. Front. Behav. Neurosci. 11.

Noble, E.E., Hsu, T.M., Liang, J., Kanoski, S.E., 2019. Early-life sugar consumption has long-term negative effects on memory function in male rats. Nutr. Neurosci. 22, 273–283.

Noble, E.E., Olson, C.A., Davis, E., Tsan, L., Chen, Y.-W., Schade, R., Liu, C., Suarez, A., Jones, R.B., De La Serre, C., Yang, X., Hsiao, E.Y., Kanoski, S.E., 2021. Gut microbial taxa elevated by dietary sugar disrupt memory function. Transl. Psychiatry 11.

Olson, C.A., Iñiguez, A.J., Yang, G.E., Fang, P., Pronovost, G.N., Jameson, K.G., Rendon, T.K., Paramo, J., Barlow, J.T., Ismagilov, R.F., Hsiao, E.Y., 2021. Alterations in the gut microbiota contribute to cognitive impairment induced by the ketogenic diet and hypoxia. Cell Host Microbe 29, 1378–1392.e1376.

Patel, H., McIntire, J., Ryan, S., Dunah, A., Loring, R., 2017. Anti-inflammatory effects of astroglial α7 nicotinic acetylcholine receptors are mediated by inhibition of the NF-κB pathway and activation of the Nrf2 pathway. J. Neuroinflammation 14, 192.

Pavlov, V.A., Tracey, K.J., 2005. The cholinergic anti-inflammatory pathway. Brain Behav. Immun. 19, 493–499.

Pepeu, G., Giovannini, M.G., 2010. Cholinesterase inhibitors and memory. Chem. Biol. Interact. 187, 403–408.

Quinn, R., 2005. Comparing rat's to human's age: how old is my rat in people years? Nutrition 21, 775.

Rothwell, N.J., Stock, M.J., 1982. Effects of feeding a palatable 'cafeteria' diet on energy balance in young and adult lean (+/?) Zucker rats. Br. J. Nutr. 47, 461–471.

Savastano, D.M., Covasa, M., 2005. Adaptation to a high-fat diet leads to hyperphagia and diminished sensitivity to cholecystokinin in rats. J. Nutr. 135, 1953–1959.

Sengupta, P., 2013. The laboratory rat: relating its age with human's. Int. J. Prev. Med. 4, 624–630.

Shively, C.A., Appt, S.E., Vitolins, M.Z., Uberseder, B., Michalson, K.T., Silverstein-Metzler, M.G., Register, T.C., 2019. Mediterranean versus Western diet effects on caloric intake, obesity, metabolism, and hepatosteatosis in nonhuman primates. Obesity 27, 777–784.

Shytle, R.D., Mori, T., Townsend, K., Vendrame, M., Sun, N., Zeng, J., Ehrhart, J., Silver, A.A., Sanberg, P.R., Tan, J., 2004. Cholinergic modulation of microglial activation by α7 nicotinic receptors. J. Neurochem. 89, 337–343.

Sobesky, J.L., Barrientos, R.M., De May, H.S., Thompson, B.M., Weber, M.D., Watkins, L. R., Maier, S.F., 2014. High-fat diet consumption disrupts memory and primes elevations in hippocampal IL-1β, an effect that can be prevented with dietary reversal or IL-1 receptor antagonism. Brain Behav. Immun. 42, 22–32.

Suarez, A.N., Hsu, T.M., Liu, C.M., Noble, E.E., Cortella, A.M., Nakamoto, E.M., Hahn, J. D., De Lartigue, G., Kanoski, S.E., 2018. Gut vagal sensory signaling regulates hippocampus function through multi-order pathways. Nat. Commun. 9, 2181.

Subramanian, K.S., Lauer, L.T., Hayes, A.M.R., Décarie-Spain, L., McBurnett, K., Nourbash, A.C., Donohue, K.N., Kao, A.E., Bashaw, A.G., Burdakov, D., Noble, E.E., Schier, L.A., Kanoski, S.E., 2023. Hypothalamic melanin-concentrating hormone neurons integrate food-motivated appetitive and consummatory processes in rats. Nat. Commun. 14.

Sullivan, P.M., 2020. Influence of Western diet and APOE genotype on Alzheimer's disease risk. Neurobiol. Dis. 138, 104790.

Swanson, L.W., 2018. Brain maps 4.0-structure of the rat brain: an open access atlas with global nervous system nomenclature ontology and flatmaps. J. Comput. Neurol. 526, 935–943.

Tap, J., Furet, J.P., Bensaada, M., Philippe, C., Roth, H., Rabot, S., Lakhdari, O., Lombard, V., Henrissat, B., Corthier, G., 2015. Gut microbiota richness promotes its stability upon increased dietary fibre intake in healthy adults. Environ. Microbiol. 17, 4954–4964.

Tran, D.M.D., Westbrook, R.F., 2017. A high-fat high-sugar diet-induced impairment in place-recognition memory is reversible and training-dependent. Appetite 110, 61–71.

Tsan, L., Chometton, S., Hayes, A.M.R., Klug, M.E., Zuo, Y., Sun, S., Bridi, L., Lan, R., Fodor, A.A., Noble, E.E., Yang, X., Kanoski, S.E., Schier, L.A., 2022a. Early life low-calorie sweetener consumption disrupts glucose regulation, sugar-motivated behavior, and memory function in rats. JCI Insight 7, e157714.

Tsan, L., Décarie-Spain, L., Noble, E.E., Kanoski, S.E., 2021. Western diet consumption during development: setting the stage for neurocognitive dysfunction. Front. Neurosci. 15.

Tsan, L., Sun, S., Hayes, A.M.R., Bridi, L., Chirala, L.S., Noble, E.E., Fodor, A.A., Kanoski, S.E., 2022b. Early life Western diet-induced memory impairments and gut microbiome changes in female rats are long-lasting despite healthy dietary intervention. Nutr. Neurosci. 25, 2490–2506.

Unger, A.L., Eckstrom, K., Jetton, T.L., Kraft, J., 2019. Colonic bacterial composition is sex-specific in aged CD-1 mice fed diets varying in fat quality. PLoS One 14, e0226635.

Wang, H., Yu, M., Ochani, M., Amella, C.A., Tanovic, M., Susarla, S., Li, J.H., Wang, H., Yang, H., Ulloa, L., Al-Abed, Y., Czura, C.J., Tracey, K.J., 2003. Nicotinic acetylcholine receptor α7 subunit is an essential regulator of inflammation. Nature 421, 384–388.

Wieckowska-Gacek, A., Mietelska-Porowska, A., Wydrych, M., Wojda, U., 2021. Western diet as a trigger of Alzheimer's disease: from metabolic syndrome and systemic inflammation to neuroinflammation and neurodegeneration. Ageing Res. Rev. 70, 101397.

Wilson, C.R., Tran, M.K., Salazar, K.L., Young, M.E., Taegtmeyer, H., 2007. Western diet, but not high fat diet, causes derangements of fatty acid metabolism and contractile dysfunction in the heart of Wistar rats. Biochem. J. 406, 457–467.

Yang, Y., Zhong, Z., Wang, B., Xia, X., Yao, W., Huang, L., Wang, Y., Ding, W., 2019. Early-life high-fat diet-induced obesity programs hippocampal development and cognitive functions via regulation of gut commensal akkermansia muciniphila. Neuropsychopharmacology 44, 2054–2064.

Zhang, Z., Hyun, J.E., Thiesen, A., Park, H., Hotte, N., Watanabe, H., Higashiyama, T., Madsen, K.L., 2020. Sex-specific differences in the gut microbiome in response to dietary fiber supplementation in IL-10-deficient mice. Nutrients 12, 2088.

Zhu, P.K., Zheng, W.S., Zhang, P., Jing, M., Borden, P.M., Ali, F., Guo, K., Feng, J., Marvin, J.S., Wang, Y., Wan, J., Gan, L., Kwan, A.C., Lin, L., Looger, L.L., Li, Y., Zhang, Y., 2020. Nanoscopic visualization of restricted nonvolume cholinergic and monoaminergic transmission with genetically encoded sensors. Nano Lett. 20, 4073–4083.